

Chiral Anomaly in $SU(2)_R$ -Axion Inflation and the New Prediction for Particle Cosmology

Azadeh Maleknejad

Theoretical Physics Department, CERN, 1211 Geneva 23, Switzerland

E-mail: azadeh.maleknejad@cern.ch

ABSTRACT: Upon embedding the axion-inflation in the minimal left-right symmetric gauge extension of the SM with gauge group $SU(2)_L \times SU(2)_R \times U(1)_{B-L}$, [arXiv:2012.11516] proposed a new particle physics model for inflation. In this work, we present a more detailed analysis. As a compelling consequence, this setup provides a new mechanism for simultaneous baryogenesis and right-handed neutrino creation by the chiral anomaly of W_R in inflation. The lightest right-handed neutrino is the dark matter candidate. This setup has two unknown fundamental scales, i.e., the scale of inflation and left-right symmetry breaking $SU(2)_R \times U(1)_{B-L} \rightarrow U(1)_Y$. Sufficient matter creation demands the left-right symmetry breaking scale happens shortly after the end of inflation. Interestingly, it prefers left-right symmetry breaking scales above 10^{10} GeV , which is in the range suggested by the non-supersymmetric $SO(10)$ Grand Unified Theory with an intermediate left-right symmetry scale. Although W_R gauge field generates equal amounts of right-handed baryons and leptons in inflation, i.e. $B - L = 0$, in the Standard Model sub-sector $B - L_{SM} \neq 0$. A key aspect of this setup is that $SU(2)_R$ sphalerons are never in equilibrium, and the primordial $B - L_{SM}$ is conserved by the Standard Model interactions. This setup yields a deep connection between CP violation in physics of inflation and matter creation (visible and dark); hence it can naturally explain the observed coincidences among cosmological parameters, i.e., $\eta_B \simeq 0.3P_\zeta$ and $\Omega_{DM} \simeq 5\Omega_B$. The new mechanism does not rely on the largeness of the unconstrained CP-violating phases in the neutrino sector nor fine-tuned masses for the heaviest right-handed neutrinos. The $SU(2)_R$ -axion inflation comes with a cosmological smoking gun; chiral, non-Gaussian, and blue-tilted gravitational wave background, which can be probed by future CMB missions and laser interferometer detectors.

Contents

1	Introduction	1
2	Framework	5
2.1	SU(2) _R -Axion Inflation	6
3	Inflationary Particle Production	8
3.1	Scenario Type-I	9
3.2	Scenario Type-II	11
3.3	Baryon and Lepton Numbers	15
4	Post Reheating Evolution	16
4.1	Thermal Evolution	16
4.2	Spectator Effects, RHN decay, and Matter Asymmetry	20
5	Modern Era Baryon Asymmetry and Dark Matter	23
5.1	Baryon to Photon Ratio	24
5.2	Right-handed Neutrino as Cold Dark Matter	25
6	Quick on Observational Constraints and Signatures	26
7	Conclusions	27
A	Overview of Minimal Left-Right Symmetric Theories	29
B	Massive Sterile Neutrino production in Inflation	35
C	Phenomenological Model of Reheating	36
C.1	Entropy Injection	38
D	Spectator Effects	39
D.1	$\mathbf{W}_{L,R}$ Sphalerons	39
D.2	Lepton Flavor Effects	40

1 Introduction

Modern cosmology has been remarkably successful in describing the Universe from a second after the Big Bang until today. However, its physics before that time is still much less certain. It profoundly involves particle theory beyond the Standard Model (BSM) to explain long-standing puzzles: I) the origin of the observed matter asymmetry, II) neutrino mass, III) nature of dark matter, and IV) cosmic inflation. Apart from the above problems, the

standard model of particle physics (SM) faces some conceptual issues: i) ad hoc parity violation, ii) accidental $B - L$ global symmetry, iii) vacuum instability, and iv) strong CP problem.

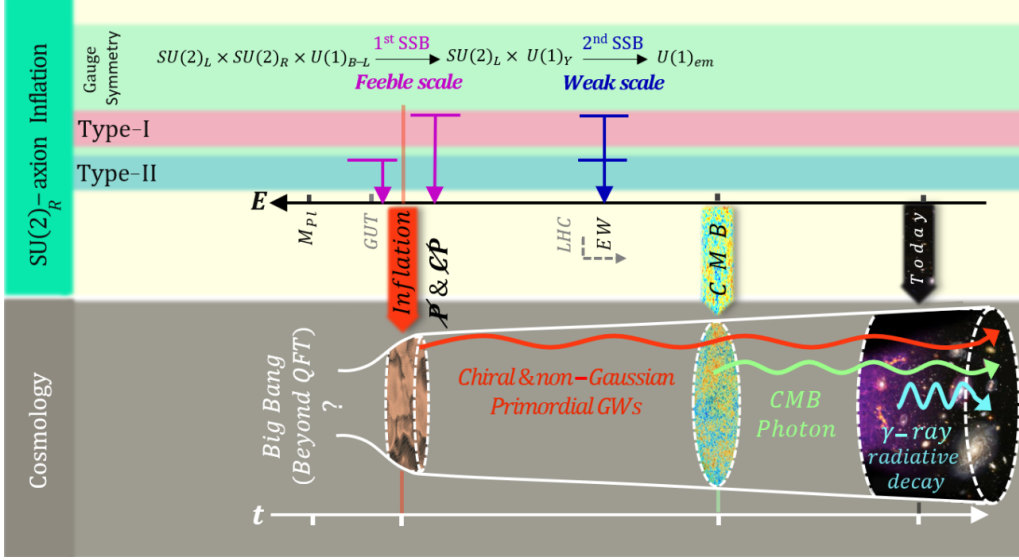


Figure 1. The $SU(2)_R$ -axion inflation throughout cosmic history. This setup has two new fundamental scales, scale of inflation $\Lambda_{\text{inf}} = \sqrt{H M_{\text{Pl}}}$, and scale of first SSB, Λ_F . Scenarios with $\Lambda_{\text{inf}} > \Lambda_F$ ($\Lambda_{\text{inf}} < \Lambda_F$) are called type-I (type-II).

Recently, [1] proposed a new setup for physics of inflation by embedding axion inflation in $SU(2)_R$ gauge extensions of the SM. For concreteness, as the most minimal realization of this idea ¹, the axion inflaton is coupled to $SU(2)_R$ gauge field in the minimal left-right symmetric model (LRSM) [2–5]. This new particle physics model for inflation gives rise to a new mechanism for simultaneous baryogenesis and Right-Handed Neutrino (RHN) creation through the chiral anomaly of $SU(2)_R$, which provides the source of CP violation in inflation. This new mechanism does not rely on the largeness of the unconstrained CP-violating phases in the neutrino sector nor fine-tuned masses for the heaviest right-handed neutrinos. On the other hand, it makes a deep connection between inflation, baryon asymmetry, and DM relic density. Therefore, it can naturally explain the observed coincidences among cosmological parameters, i.e., $\eta_B \simeq 0.3 P_\zeta$ and $\Omega_{DM} \simeq 5 \Omega_B$. If the primordial relic density of the lightest RHN makes all the DM today, Ω_{DM} specifies its mass as 1.7 GeV . Therefore its radiative decay may produce active neutrinos and gamma-rays with energy $E_\gamma = m_{N_1}/2$ in the highly-dense DM regions. As a compelling consequence, this setup can simultaneously provide plausible explanations for the phenomena (I-IV) named earlier. In this work, we present a more detailed analytical and numerical analysis.

Originally proposed to explain P violation in low energy processes [2], LRSM predicted massive neutrinos years before experiment. Among its additional compelling consequences are: natural $B - L$ symmetry [6], natural entailed seesaw mechanisms [7], solution to vacuum

¹This is the minimal realization that can produce a non-zero $B - L$ in the SM sector, i.e. $B_{\text{SM}} - L_{\text{SM}} \neq 0$.

stability problem [8], and strong CP problem without an axion. The LRSM can solve the conceptual issues (i-iv) named earlier. In the minimal LRSM, the Electro-Weak (EW) gauge symmetry is extended to $SU(2)_L \times SU(2)_R \times U(1)_{B-L}$ [2–5]. As a result, it introduces a new fundamental scale, Λ_F , during which the extended gauge symmetry is broken as $SU(2)_R \times U(1)_{B-L} \rightarrow U(1)_Y$. Upon embedding axion-inflation in LRSM, we have two unknown energy scales, the scale of inflation and Λ_F . Based on that we can classify the setup into two types; type-I with $\sqrt{HM_{Pl}} > \Lambda_F$ and type-II with $\sqrt{HM_{Pl}} < \Lambda_F$. (See Fig. 1)

Axion fields are abundant in string theory, and therefore very well-motivated candidates for the inflaton field [9–11]. Thanks to their natural shift symmetry, their effective potential is protected from dangerous quantum corrections, which guarantees the flatness of the potential. Besides their appealing theoretical stability, models of axion inflation are attractive phenomenologically and are naturally coupled to gauge fields. Non-Abelian gauge fields may contribute to the physics of inflation while respecting the cosmological symmetries [12, 13]. The first inflationary model based on non-Abelian gauge fields has been introduced as Gauge-flation [12], which is an EFT of a larger model, i.e., Chromo-natural [14], after integrating out the axion [15].² Inspired by the original models, several more inflationary models with the $SU(2)$ fields have been proposed and studied, which share the same key features. In this work, we consider the minimal realization of $SU(2)$ -axion inflation introduced and studied in [17]. For review see [18], Sec. 2 of [19] and references therein. Including $SU(2)$ gauge fields in physics of inflation give rise to a rich phenomenology which we summarize in the following. The $SU(2)$ -axion inflation [17] is a natural setting for warm inflation [20–22]. The Chern-Simons interaction drains kinetic energy from the axion and injects it into the radiation. This gauge field produces particles in inflation; charged Higgs via the Schwinger effect [23] and charged fermions by both Schwinger effect and chiral anomaly [1, 24, 25]. Another consequence of this Schwinger effect is sourced primordial gravitational waves [19]. All the Sakharov conditions [26] are satisfied in inflation [27, 28], hence it provides a natural setting to explain the matter asymmetry (see Sec. 3.3).³ As a cosmological smoking gun, it predicts chiral [18, 31, 32] and non-Gaussian [33] Gravitational Wave Background (GWB) which leads to parity odd CMB cross-spectra (see [34] and Sec. 6) [35].

The new setup proposed in [1] extended the field content of the minimal LRSM with an axion field which drives the cosmic inflation. It is assumed that the axion and $SU(2)_R$ gauge field are coupled by a Chern-Simons interaction, i.e., $SU(2)_R$ -axion inflation.⁴ Here

²In Chromo-natural, the form of the axion potential is assumed to be cosine, which requires a large value of λ to support slow-roll inflation [14]. However, the large coupling is hard to achieve in a controlled string compactification [16]. Therefore, we are interested in flat axion potentials and small values of λ , e.g. $f \lesssim 0.01$ and $\lambda \lesssim 0.1$ [17].

³Within the SM and through (global) gravitational anomaly, this setting naturally accompanies an inflationary leptogenesis [28–30].

⁴In principle we can couple the axion to both $SU(2)_R$ and $SU(2)_L$ gauge fields. However, any primordial left-handed baryons and leptons produced by $SU(2)_L$ (i.e. $B_{SM} = L_{SM}$) will be completely washed out by the $SU(2)_L$ sphaleon effects which are in thermal equilibrium between T_{reh} and m_{WL} . Therefore in the minimal realization of this idea we neglect this interaction.

both Parity and CP are spontaneously violated by the axion and its interaction with \mathbf{W}_R in the physics of inflation. Within this setup, $SU(2)_R$ gauge field is generated in inflation and creates right-handed chiral fermions coupled to it, i.e., SM baryons \mathbf{B} , SM leptons \mathbf{L}_{SM} , and three Right-Handed Neutrinos (RHN) \mathbf{L}_N . In type-I scenario in which the first SSB happens after inflation, equal baryon and lepton numbers are created in inflation, i.e. $\mathbf{B} = \mathbf{L}$ where $\mathbf{L} \equiv \mathbf{L}_{\text{SM}} + \mathbf{L}_N$, yet $\mathbf{B} - \mathbf{L}_{\text{SM}} \neq 0$. Shortly after inflation, the first SSB happens at Λ_F , and eventually, the $SU(2)_R$ interactions freeze out at temperature T_{W_R} . The lightest of RHNs with feeble Yukawa couplings (our DM candidate) is decoupled at this point, while $N_{2,3}$ decay at $T = m_{N_{2,3}}$. Between reheating and EW scale, the spectator effects reshuffle the primordial densities. The summary of this new mechanism for simultaneous baryogenesis and RHN production is presented in Fig. 2. Ref. [1] was the first step to further, more involved analysis on the rich and multifaceted phenomenology of the gauge extensions of the SM in inflation physics. In the current work, we present a more detailed analytical and numerical analysis of the setup.

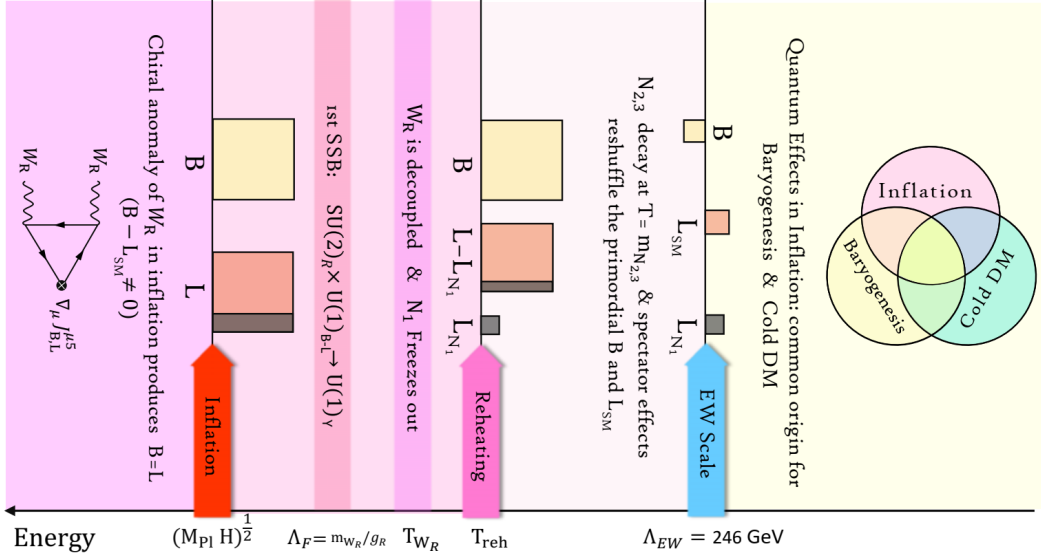


Figure 2. Summary of the mechanism: Illustration shows the evolution of baryons \mathbf{B} (yellow box), SM leptons \mathbf{L}_{SM} (pink box) and RHNs $\mathbf{L}_N = \sum_{i=1}^3 \mathbf{L}_{N_i}$ (gray box) during cosmic evolution. Here $\mathbf{B} \equiv \mathbf{B}_{\text{SM}}$ and $\mathbf{L} \equiv \mathbf{L}_{\text{SM}} + \mathbf{L}_N$. The CP violation by the chiral anomaly of W_R in inflation simultaneously produces baryons, SM leptons, and RHNs in inflation. The lightest RHN (our DM candidate N_1) freezes out at $T = T_{W_R}$. Between reheating and electroweak scale, the spectator effects reshuffle the primordial densities while $N_{2,3}$ decay at $T = m_{N_{2,3}}$. The net baryon density and dark matter today are the remnant of that quantum effect in inflation. Notice that $T_{\text{reh}} < m_{W_R}$ condition is essential to keep W_R sphalerons out of equilibrium (see App D.1). The W_L sphalerons, however, contribute to the spectator effects and washout $\mathbf{B} + \mathbf{L}_{\text{SM}}$ but conserve $\mathbf{B} - \mathbf{L}_{\text{SM}}$.

The paper is structured as follows. In Sec. 2 we review the setup of $SU(2)_R$ -axion inflation embedded in LRSM. In Sec. 3, we work out the inflationary particle production. In Sec. 4, we study the post reheating evolution of the system. Next in Sec. 5, we work out the final baryon asymmetry and dark matter in the modern era. Sec. 6 presents a quick

discussion on the setup's observational constraints and signatures. We finally conclude in Sec. 7. Technical details of the computations and the underlying mathematical tools are provided in App.s A-D.

Notations and conventions: In this work, we deal with 4 and 2-component spinors, which are acted upon by 4×4 and 2×2 matrices, respectively. The 4-spinors and 4×4 matrices are remained unchanged, while the 2-spinors and 2×2 matrices are written in boldface. The 2×2 identity matrix is represented as \mathbf{I}_2 . L and R subscripts denote the left- and right-handed fermions. The lepton and baryon numbers are presented by \mathbf{L} and \mathbf{B} . The Hubble parameter in inflation is denoted by H and $M_{\text{Pl}} = (8\pi G)^{-1}$ is set to one, unless otherwise specified. We use the Einstein summation notation, i.e., repeated indices (one upper and one lower) are summed. The beginning of the Latin alphabets, i.e. a, b, c denote the $SU(2)$ group indices. Greek letters starting from the middle of the alphabet, i.e., μ, ν, \dots are used for the space-time indices, whereas the starting ones, i.e., α, β, \dots , present the indices of the tangent space (non-coordinate) bases.

2 Framework

The aim of this work is to embed the axion inflation in the gauge extensions of the SM when the inflaton is directly coupled to the BSM fields. Here we consider the model proposed in [1], i.e. $SU(2)_R$ -axion inflation, in which the axion-inflation is embedded in the minimal Left-Right Symmetric Model (LRSM). The minimal gauge group that implements the hypothesis of left-right symmetry is [2–5]

$$\mathcal{G} \equiv SU(2)_L \times SU(2)_R \times U(1)_{\mathbf{B-L}}, \quad (2.1)$$

where the color ($SU(3)$ group) is suppressed. The subscripts L and R denotes left- and right-handed fields, while \mathbf{B} and \mathbf{L} represent baryon and lepton numbers respectively. The LRSM includes three gauge fields; $\mathbf{W}_{L,R}$ are associated with $SU(2)_{L,R}$ and B_μ corresponds to $U(1)_{\mathbf{B-L}}$. The fermionic content consists of the SM quarks and leptons extended by three RHNs as

$$q_{iL,R} = \begin{pmatrix} \mathbf{u}_i \\ \mathbf{d}_i \end{pmatrix}_{L,R} \quad \text{and} \quad l_{iL,R} = \begin{pmatrix} \boldsymbol{\nu}_i \\ l_i \end{pmatrix}_{L,R}, \quad (2.2)$$

where $\boldsymbol{\nu}_{iR}$ are three RHNs. The right-handed fermions interact with \mathbf{W}_R gauge field which is $SU(2)_R$ -valued, and is given as

$$\mathbf{W}_R = W_R^a \mathbf{T}_a \quad \text{and} \quad [\mathbf{T}_a, \mathbf{T}_b] = i\epsilon_{abc} \mathbf{T}_c. \quad (2.3)$$

The extended Higgs sector of the model consists of a Higgs bi-doublet $\boldsymbol{\Phi}$, and $SU(2)_{L,R}$ triplets $\boldsymbol{\Delta}_{L,R}$. The Spontaneous Symmetry Breaking (SSB) structure is

$$SU(2)_L \times SU(2)_R \times U(1)_{\mathbf{B-L}} \xrightarrow[\text{1st SSB}]{T < \Lambda_F} SU(2)_L \times U(1)_Y \xrightarrow[\text{2nd SSB}]{T < \Lambda_W} U(1)_{em}.$$

The first SSB occurs at $T = \Lambda_F$ which breaks the left-right symmetry and gives a VEV to the $SU(2)_R$ triplet, i.e. $\langle \boldsymbol{\Delta}_R \rangle \neq 0$. That gives mass to W_R^\pm , Z_R , and provides Majorana

masses for $\mathbf{N}_i \equiv \boldsymbol{\nu}_i + \boldsymbol{\nu}_i^c$. Next, when the temperature gets below EW scale, $T < \Lambda_W$, the second SSB happens, and the Higgs bi-doublet acquires a VEV, i.e., $\langle \Phi \rangle \neq 0$. It gives Dirac masses to the SM particles, active neutrinos included. In the minimal LRSM, the origin of the mass for the SM neutrino is a hybrid (I+II) seesaw mechanism [7]. For an overview on LRSM, see Appendix A and the references therein.

2.1 $SU(2)_R$ -Axion Inflation

Cosmic inflation is given by Friedmann-Lemaître-Robertson-Walker (FLRW) metric

$$ds^2 = -dt^2 + a^2(t)\delta_{ij}dx^i dx^j, \quad (2.4)$$

in which the Hubble parameter is almost constant $H(t) \simeq H$, and the scale factor is $a(t) \simeq e^{Ht}$. As for the inflaton field we consider an axion field φ which is coupled to the \mathbf{W}_R gauge field in the LRSM as [1]

$$\mathcal{L}_{Inf} = -\frac{1}{2}\partial_\mu\varphi^2 - V(\varphi) - \frac{1}{2}\text{Tr}[\mathbf{W}_{R\mu\nu}\mathbf{W}_R^{\mu\nu}] - \frac{\lambda\varphi}{f}\text{Tr}[\mathbf{W}_{R\mu\nu}\tilde{\mathbf{W}}_R^{\mu\nu}], \quad (2.5)$$

where $\lambda \lesssim 1$ is a dimensionless parameter, $f \lesssim 10^{-1}M_{\text{Pl}}$ is the axion decay constant, $\mathbf{W}_R^{\mu\nu}$ is the strength tensor of \mathbf{W}_R^μ as

$$\mathbf{W}_{R\mu\nu} \equiv \partial_\mu\mathbf{W}_{R\nu} - \partial_\nu\mathbf{W}_{R\mu} - ig_R[\mathbf{W}_{R\mu}, \mathbf{W}_{R\nu}], \quad (2.6)$$

and $\tilde{\mathbf{W}}_R^{\mu\nu} \equiv \frac{1}{2}\frac{\epsilon^{\mu\nu\lambda\sigma}}{\sqrt{-g}}\mathbf{W}_{R\lambda\sigma}$. For the sake of generality, we assume $V(\varphi)$ is an arbitrary axion potential, flat enough to support the slow-roll inflation. This $SU(2)$ -axion inflation model and its cosmic perturbations, for a generic dark $SU(2)$ field, has been introduced and studied in [17] (See also [28, 29]). One of the most popular and well-motivated axion models of inflation to provide the flat potential is the axion monodromy. While the underlying periodicity of the theory continues to protect the inflaton potential from corrections, here the periodic field space of the axion is effectively unfolded due to the monodromy [11, 36, 37].

In this setup, we have two unknown high energy scales, i.e., the scale of inflation $\Lambda_{inf} = \sqrt{M_{\text{Pl}}H}$, and LR symmetry breaking scale Λ_F . Besides, the $SU(2)_R$ may or may not acquire a VEV. Therefore, we can distinguish four different types of scenarios, which are classified in Table 1. Scenario **I** and **I_v** describe the case $\Lambda_{inf} > \Lambda_F$, while **II** and **II_v** otherwise, i.e. $\Lambda_{inf} < \Lambda_F$. Moreover, the v subscript denotes systems in which the $SU(2)_R$ acquires a VEV in inflation. In scenarios **II** and **II_v**, the \mathbf{W}_R is massive in inflation.⁵ In this work we solely focus on types **I** and **II** and leave **I_v** and **II_v** for future work.

⁵For different but related models based on massive $SU(2)$ fields coupled to an $SU(2)$ -doublet see [38, 39].

	$\Lambda_{inf} > \Lambda_F$	$\Lambda_{inf} < \Lambda_F$
$\langle \mathbf{W}_R \rangle = 0$	I	II
$\langle \mathbf{W}_R \rangle \neq 0$	I_v	II_v

Table 1. Different scenarios of $SU(2)_R$ -axion inflation. Based on the scale of inflation $\Lambda_{inf} = \sqrt{M_{Pl}H}$, scale of left-right symmetry breaking Λ_F , and the (possible) $SU(2)_R$ field's VEV in inflation, one can separate four different types of scenarios.

Right-handed fermions in $SU(2)_R$ -axion inflation:

The $U(1)_{B-L}$ and $SU(2)_L$ gauge fields and left-handed fermions in inflation have conformal symmetry, hence are negligible in physics of inflation. The \mathbf{W}_R gauge field, however, is coupled to the axion which breaks its conformal symmetry and sources it in inflation. The right-handed fermions are coupled to \mathbf{W}_R as (see Eq. (A.14)) ⁶

$$\mathcal{L} \supset \sum_i \bar{q}_{iR} (i\sigma^\mu D_\mu - ig_R \sigma^\mu \mathbf{W}_{R\mu}) q_{iR} + \bar{l}_{iR} (i\sigma^\mu D_\mu - ig_R \sigma^\mu \mathbf{W}_{R\mu}) l_{iR}, \quad (2.7)$$

where D_μ is the spinor covariant derivative. The generated \mathbf{W}_R gauge field, hence, produces right-handed quarks and leptons in inflation. Finally, the right-handed fermions can have an effective interaction with the axions as

$$\mathcal{L}_5 = \frac{\tilde{\lambda}\varphi}{f} \nabla_\mu J_R^\mu, \quad (2.8)$$

where $\tilde{\lambda}$ is a constant of the order of λ , and the right-handed current is

$$J_R^\mu = \sum_i \bar{q}_{iR} \sigma^\mu q_{iR} + \bar{l}_{iR} \sigma^\mu l_{iR}. \quad (2.9)$$

There are two source terms for the fermions, i.e. the $SU(2)_R$ gauge field and its axion. However, the axion cannot generate Weyl fermions. The reason is that a Peccei-Quinn type $U_{PQ}(1)$ rotation of fermions as [40]

$$\Psi_R \rightarrow e^{-\frac{i\tilde{\lambda}}{f}\varphi} \Psi_R, \quad (2.10)$$

removes the axion interaction and transforms the fermion mass matrix as [41]

$$\mathcal{M} \rightarrow e^{\frac{2i\tilde{\lambda}}{f}\varphi} \mathcal{M}. \quad (2.11)$$

Therefore, the axion only contributes to the generation of massive fermions in inflation.

⁶Notice that $U(1)_{B-L}$ is decaying and unimportant in inflation, and it is neglected here.

3 Inflationary Particle Production

In this inflation model, \mathbf{W}_R gauge field is generated by the axion. The field equation of $\mathbf{W}_{R\mu}$ in the massless case (type-I scenarios) is

$$(\nabla_\mu - ig_R \mathbf{W}_{R\mu})[\mathbf{W}_R^{\mu\nu} + \frac{\lambda\varphi}{f} \tilde{\mathbf{W}}_R^{\mu\nu}] = 0, \quad (3.1)$$

and in the massive case (type-II scenarios) W_R^\pm and Z_R^0 acquire m_{W_R} and m_{Z_R} respectively. Moreover, apart from the exponential expansion of the Universe, both axion and \mathbf{W}_R gauge field are active in inflation and produce right-handed quarks and leptons. The P and C are maximally broken by the chiral nature of the $SU(2)_R$ interaction, and CP is violated by the Chern-Simons interaction. Both right-handed baryon and lepton numbers are violated by the non-perturbative effects of the \mathbf{W}_R , i.e. chiral (Adler-Bell-Jackiw) anomaly [42, 43]. The sterile neutrinos are massless (massive with mass m_{N_i}) in scenario type-I (type-II). That gives the right-handed baryons and leptons the following anomalies

$$\nabla_\mu J_B^{\mu R} = -\frac{g_R^2 \mathcal{N}_R}{16\pi^2} \text{Tr}[\mathbf{W}_R^{\mu\nu} \tilde{\mathbf{W}}_{R\mu\nu}], \quad (3.2)$$

$$\nabla_\mu J_L^{\mu R} = -\frac{g_R^2 \mathcal{N}_R}{16\pi^2} \text{Tr}[\mathbf{W}_R^{\mu\nu} \tilde{\mathbf{W}}_{R\mu\nu}] + 2im_{N_i} \bar{\nu}_{iR} \nu_{iR}, \quad (3.3)$$

where $J_{B,L}^{\mu R}$ is the baryon and lepton number densities, and \mathcal{N}_R is the number of right-handed fermion generations. Note that the B and L violating interactions of the left-handed fermions remains negligible in inflation. The Chern-Simons term can be written as a total derivative

$$\sqrt{-g} \text{Tr}[\mathbf{W}_R^{\mu\nu} \tilde{\mathbf{W}}_{R\mu\nu}] = 2\partial_\mu (\sqrt{-g} K^\mu), \quad (3.4)$$

where K_μ is the Chern-Simons current, i.e.

$$K^\mu = \epsilon^{\mu\nu\lambda\sigma} \text{Tr}[\mathbf{W}_{R\nu} \partial_\lambda \mathbf{W}_{R\sigma} - \frac{2ig_R}{3} \mathbf{W}_{R\nu} \mathbf{W}_{R\lambda} \mathbf{W}_{R\sigma}]. \quad (3.5)$$

In our setup $\mathcal{N}_L = \mathcal{N}_R = 3$, hence we neglect the effect of global gravitational anomaly.⁷ The total baryon and lepton numbers are related to their corresponding quantities in SM as

$$n_B = n_{B_{\text{SM}}} \quad \text{and} \quad n_L = n_{L_{\text{SM}}} + \sum_i n_{N_i}, \quad (3.6)$$

in which $n_{L_{\text{SM}}}$ and n_{N_i} are the contributions of the SM leptons and the i th RHN in the total lepton number respectively. In this section, $g_{L,R}$ are the gauge couplings at the scale of inflation which are computed in App. A. For a high scale inflation, e.g. around $H \sim 10^{14}$ GeV, we have

$$g_L(H) \simeq 0.56 \quad \text{and} \quad 0.3 \leq g_L(H) \leq 0.56. \quad (3.7)$$

⁷In the context of Einstein gravity and with SM fermions, i.e. $\mathcal{N}_L - \mathcal{N}_R = 3$, the effect of global gravitational leptogenesis in the minimal $SU(2)$ -axion model [17] is studied in [28, 29].

The details of the discussion depend on whether the first SSB happens before or after inflation. Therefore, these two cases will be treated separately. Before going any further, let us fix the notations that will be used in this section. For later convenience, we define \mathcal{H} as

$$\mathcal{H} \equiv aH, \quad (3.8)$$

which in terms of conformal time, i.e. $dt = ad\tau$, and during slow-roll is $\mathcal{H} \simeq -\frac{1}{\tau}$. The rescaled physical momentum is defined as

$$\tilde{\tau} \equiv \frac{k}{aH} \simeq -k\tau. \quad (3.9)$$

Finally, we define dimensionless parameters ξ and $\tilde{\xi}$ as

$$\xi \equiv \frac{\lambda\dot{\phi}}{2fH} \quad \text{and} \quad \tilde{\xi} \equiv \frac{\tilde{\lambda}}{\lambda}\xi. \quad (3.10)$$

During slow-roll ξ has slow-roll dynamics, and is related to the slow-roll parameter $\epsilon \equiv -\frac{\dot{H}}{H^2}$ as

$$\xi(t) \sim \frac{1}{\sqrt{2}} \frac{\lambda M_{\text{Pl}}}{fH} \sqrt{\epsilon(t)}. \quad (3.11)$$

As a result, ξ gradually increases with time.

3.1 Scenario Type-I

In scenario type-I, the \mathbf{W}_R and right-handed fermions are all massless in inflation. Here we first study the gauge field production by the axion. Next, we turn to the fermion production by the gauge field.

Massless $\text{SU}(2)_R$ gauge bosons:

The linearized field equation of $SU(2)_R$ is

$$\partial_\tau^2 \mathbf{W}_{Ri} - \partial_j^2 \mathbf{W}_{Ri} + a^2 \partial_i (\nabla_\mu \mathbf{W}_R^\mu) + 2a\mathcal{H} \partial_i \mathbf{W}_{R0} - \frac{\lambda\dot{\phi}}{fH} \epsilon^{ijk} \mathcal{H} \partial_j \mathbf{W}_{Rk} \simeq 0, \quad (3.12)$$

and a constraint equation $\nabla_\mu \mathbf{W}_R^\mu = 0$. The (charged) gauge field has two degrees of freedoms and can be decomposed in terms of its two transverse modes as

$$\mathbf{W}_{Ri}(\tau, \mathbf{x}) = \sum_{\sigma=\pm 1} \int d^3k \left(a_{\mathbf{k},\sigma} \mathbf{f}_\sigma(\tau, \mathbf{k}) e_{\sigma i}(\mathbf{k}) e^{i\mathbf{k}\cdot\mathbf{x}} + b_{\mathbf{k},\sigma}^\dagger \mathbf{f}_\sigma^*(\tau, \mathbf{k}) e_{\sigma i}^*(\mathbf{k}) e^{-i\mathbf{k}\cdot\mathbf{x}} \right), \quad (3.13)$$

where $a_{\mathbf{k},\sigma}$ ($b_{\mathbf{k},\sigma}$) is the annihilation operator of the particle (anti-particle), and $\mathbf{e}_\pm(\mathbf{k})$ are ± 1 helicity polarization vectors, defined as

$$\mathbf{e}_\pm(\mathbf{k}) \equiv \frac{1}{\sqrt{2}} (\hat{\boldsymbol{\theta}} \mp i\hat{\boldsymbol{\phi}}), \quad (3.14)$$

where $\hat{\mathbf{r}} = -\hat{\mathbf{k}}$, $\hat{\boldsymbol{\theta}}$ and $\hat{\boldsymbol{\phi}}$ are the local orthogonal unit vectors in the directions of increasing r , θ , and ϕ . The polarization vectors satisfy in the following equations

$$\mathbf{k} \cdot \mathbf{e}_{\pm}(\mathbf{k}) = 0 \quad \text{and} \quad \mathbf{k} \times \mathbf{e}_{\pm}(\mathbf{k}) = \mp i k \mathbf{e}_{\pm}(\mathbf{k}). \quad (3.15)$$

The function $\mathbf{f}_{\sigma}(\mathbf{k})$ can be expanded in terms of the mode functions as

$$\mathbf{f}_{\sigma}(\tau, \mathbf{k}) = f_{\sigma}^a(\tau, \mathbf{k}) \mathbf{T}_a, \quad (3.16)$$

which are governed by the field equations below

$$\partial_{\tau}^2 f_{\pm}^a + (k^2 \mp 2k\mathcal{H}\xi) f_{\pm}^a \simeq 0. \quad (3.17)$$

The field equation can be written as a Whittaker equation with parameters

$$\kappa_{\pm} = \mp i\xi \quad \text{and} \quad \mu^2 = \frac{1}{4}. \quad (3.18)$$

Imposing the Bunch-Davies vacuum condition in the asymptotic past, we have the mode functions as [17]

$$f_{\pm}^a(\tau, \mathbf{k}) = \frac{e^{i\kappa_{\pm}\pi/2}}{(2\pi)^{\frac{3}{2}}\sqrt{2k}} W_{\kappa_{\pm}, \mu}(2ik\tau). \quad (3.19)$$

Therefore one helicity state of the gauge field (plus/minus for positive/negative ξ) has a short period of tachyonic growth (See the left panel of Fig. 3).⁸

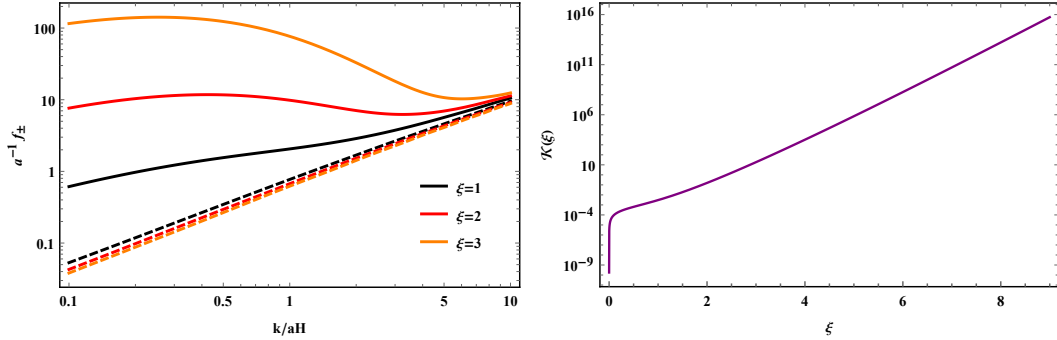


Figure 3. The $SU(2)_R$ gauge boson and right-handed fermion production in type-I scenarios. Left panel: The polarization states of the $SU(2)_R$ field vs $\frac{k}{aH}$ for different values of ξ . The plus and minus helicity states are presented with solid and dashed lines respectively. Right panel: the $\mathcal{K}(\xi)$ parameter which quantifies the value of fermion production in inflation.

Massless right-handed fermions:

In scenario type-I, all the fermions are massless in inflation. Therefore, the right-handed fermions are generated by the $SU(2)_R$ gauge field as

$$\nabla_{\mu} J_{B,L}^{\mu R} = -\frac{g_R^2 \mathcal{N}_R}{16\pi^2} \text{Tr}[\mathbf{W}_R^{\mu\nu} \tilde{\mathbf{W}}_{R\mu\nu}], \quad (3.20)$$

⁸It leads to particle production and backreaction to the background [19].

which implies that the produced right-handed fermions are given by the Chern-Simons current (3.5). After linearization, the Chern-Simons charge is given as

$$n_{\text{CS}} \equiv \int d^3k K^0 \simeq \frac{1}{a^3} \int d^3k \epsilon^{ijk} \langle \text{Tr} [\mathbf{W}_i \partial_j \mathbf{W}_k]_R \rangle. \quad (3.21)$$

For later convenience, we define $\mathcal{K}(\xi)$ as

$$\mathcal{K}(\xi) \equiv \frac{9}{4(2\pi)^4} \sum_{\sigma=\pm} \sigma e^{i\kappa_\sigma \pi} \int \tilde{\tau}^3 d \ln \tilde{\tau} W_{\kappa_\sigma, \mu}^* (-2i\tilde{\tau}) W_{\kappa_\sigma, \mu} (-2i\tilde{\tau}), \quad (3.22)$$

with $\kappa_\pm = \mp i\xi$ and $\mu = \frac{1}{2}$. Using solution (3.19), we can write n_{CS} as

$$n_{\text{CS}} \simeq \frac{8\pi^2}{3} H^3 \mathcal{K}(\xi), \quad (3.23)$$

That gives the lepton and baryon number densities as

$$n_{\text{B}} = n_{\text{L}} \simeq -g_R^2 H^3 \mathcal{K}(\xi). \quad (3.24)$$

The number density of N_i is

$$n_{\text{N}_i} = -\frac{1}{6} g_R^2 H^3 \mathcal{K}(\xi). \quad (3.25)$$

The right panel of Fig 3 shows $\mathcal{K}(\xi)$ vs ξ . It increases exponentially with the increase of ξ as

$$\mathcal{K}(\xi) \propto \frac{1}{(2\pi)^4} e^{2\xi\pi}. \quad (3.26)$$

3.2 Scenario Type-II

In scenario type-II, the gauge symmetry $SU(2)_R \times U(1)_{\text{B-L}}$ breaks to $U(1)_Y$. It gives masses to the gauge boson, charged and neutral, i.e.

$$W_R^\pm = \frac{1}{\sqrt{2}} (W_R^1 \mp iW_R^2) \quad \text{and} \quad Z_R^0 = (g_R W_R^3 - g_{\text{BL}} B) / \sqrt{g_R^2 + g_{\text{BL}}^2}, \quad (3.27)$$

as well as at least two of the right-handed fermions. Here we first study the gauge field production by the axion. Next, we turn to the fermion production by the gauge field and the axion.

Massive $SU(2)_R$ Gauge Bosons:

The linearized field equation of W_R^\pm is

$$\partial_\tau^2 W_{Ri}^\pm - \partial_j^2 W_{Ri}^\pm + a^2 \partial_i (\nabla_\mu W_R^{\pm\mu}) + 2a\mathcal{H} \partial_i W_{R0}^\pm - \frac{\lambda \dot{\varphi}}{fH} \epsilon^{ijk} \mathcal{H} \partial_j W_{Rk}^\pm + \frac{m_{W_R}^2}{H^2} \mathcal{H}^2 W_{Ri}^\pm \simeq 0, \quad (3.28)$$

with a constraint equation

$$\nabla_\mu W_R^{\pm\mu} = 0. \quad (3.29)$$

The neutral component Z_R^0 , satisfies the same equations with m_{w_R} replaced by m_{z_R} . Since the gauge field is massive, in addition to the two transverse modes with polarization vectors $\mathbf{e}^\pm(\mathbf{k})$, there is another dynamical degree of freedom associated with $k_i \mathbf{W}_R^i(\mathbf{k})$. For ease of notation, we define

$$W_R^\alpha \equiv (W_R^+, W_R^-, Z_R^0). \quad (3.30)$$

The gauge field in the massive case is given as

$$W_{Ri}^\alpha(\tau, \mathbf{x}) = \sum_{\sigma=1}^3 \int d^3k \left(a_{\mathbf{k},\sigma} f_\sigma^\alpha(\tau, \mathbf{k}) e_{\sigma i}(\mathbf{k}) e^{i\mathbf{k}\cdot\mathbf{x}} + b_{\mathbf{k},\sigma}^\dagger f_\sigma^{*\alpha}(\tau, \mathbf{k}) e_{\sigma i}^*(\mathbf{k}) e^{-i\mathbf{k}\cdot\mathbf{x}} \right), \quad (3.31)$$

where the polarization states are defined as

$$\mathbf{e}_{1,2}(\mathbf{k}) \equiv \mathbf{e}_\pm(\mathbf{k}) \quad \text{and} \quad \mathbf{e}_3(\mathbf{k}) \equiv \hat{\mathbf{k}}. \quad (3.32)$$

Note that superscript \pm denotes the charged of the field and subscript \pm represents its helicity state. In addition to these dynamical fields, massive gauge field has W_{R0}^α which is non-dynamical, specified by the constraint Eq. (3.29)

$$\partial_\tau W_{R0}^\alpha + 3\mathcal{H}W_{R0}^\alpha - \frac{1}{a}\partial_i W_{Ri}^\alpha = 0. \quad (3.33)$$

Since it is only coupled to the longitudinal mode, it can be expanded as

$$W_{R0}^\alpha(\tau, \mathbf{x}) = \frac{1}{a} \int d^3k \left(a_{\mathbf{k},3} f_0^\alpha(\tau, \mathbf{k}) e^{i\mathbf{k}\cdot\mathbf{x}} + b_{\mathbf{k},3}^\dagger f_0^{*\alpha}(\tau, \mathbf{k}) e^{-i\mathbf{k}\cdot\mathbf{x}} \right). \quad (3.34)$$

The field equation of the transverse modes with $\sigma = 1, 2$ (plus and minus helicity states) are given as

$$\partial_\tau^2 f_\pm^\alpha + (k^2 \mp 2k\mathcal{H}\xi + \frac{m_{w_R}^2}{H^2} \mathcal{H}^2) f_\pm^\alpha \simeq 0. \quad (3.35)$$

The field equation of the longitudinal mode with $\sigma = 3$ is given as

$$\partial_\tau^2 f_3^\alpha + (k^2 + \frac{m_{w_R}^2}{H^2} \mathcal{H}^2) f_3^\alpha + 2ik\mathcal{H}f_0^\alpha \simeq 0, \quad (3.36)$$

which is coupled to the W_{R0}^α is given by the constraint Eq (3.33) as

$$\partial_\tau f_0^\alpha + 2\mathcal{H}f_0^\alpha - ikf_3^\alpha = 0. \quad (3.37)$$

Like the massless case, the field equation of the transverse modes can be written as a Whitaker equation with parameters

$$\kappa_\pm = \mp i\xi \quad \text{and} \quad \mu_\alpha^2 = \frac{1}{4} - \frac{m_\alpha^2}{H^2}. \quad (3.38)$$

Imposing the Bunch-Davies vacuum condition in the asymptotic past, we have

$$f_\pm^\alpha(\mathbf{k}, \tau) = \frac{e^{i\kappa_\pm\pi/2}}{(2\pi)^{\frac{3}{2}}\sqrt{2k}} W_{\kappa_\pm, \mu_\alpha}(2ik\tau). \quad (3.39)$$

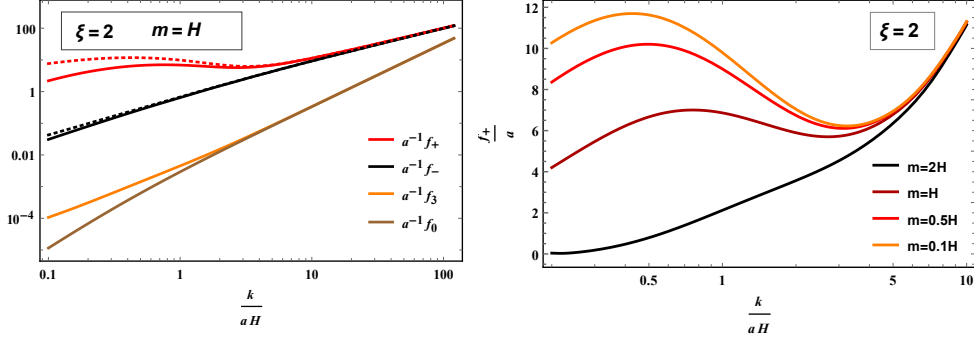


Figure 4. The polarization states of massive gauge field vs $\frac{k}{aH}$ for $\xi = 2$. Left panel shows the four components of the massive field ($\frac{f_+}{a}, \frac{f_-}{a}, \frac{f_3}{a}, \frac{f_0}{a}$) with $m = H$. The dotted lines show the corresponding modes in the massless case. Right panel shows the enhanced mode f_+ vs $\frac{k}{a}$ for different values of mass.

Since the longitudinal mode f_3^α and hence f_0^α are not coupled to the axion, they are strictly decaying and unimportant in inflation (see left panel of Fig. 4). Therefore, similar to the type-I case, the cosmologically relevant modes in type-II scenarios are the transverse modes as well. Again f_+ polarization mode is generated by the axion which is shown in the right panel of Fig. 4.

Massive right-handed neutrinos:

In scenario type-II, the SM fermions are massless in inflation while at least two of the sterile neutrinos are massive. Therefore, we have

$$\nabla_\mu J_B^\mu = -\frac{3g_R^2}{16\pi^2} \text{Tr}[\mathbf{W}^{\mu\nu} \tilde{\mathbf{W}}_{\mu\nu}]_R, \quad (3.40)$$

$$\nabla_\mu J_L^\mu = 2im_{N_i} \bar{\nu}_{iR} \nu_{iR} - \frac{3g_R^2}{16\pi^2} \text{Tr}[\mathbf{W}^{\mu\nu} \tilde{\mathbf{W}}_{\mu\nu}]_R. \quad (3.41)$$

The Chern-Simons charge given in Eq. (3.21) can be written as

$$n_{\text{CS}} \simeq \frac{8\pi^2}{9} H^3 [2\mathcal{K}(\xi, m_{W_R}) + \mathcal{K}(\xi, m_{Z_R})], \quad (3.42)$$

where $\mathcal{K}(\xi, m_\alpha)$ is

$$\mathcal{K}(\xi, m_\alpha) \equiv \frac{9}{4(2\pi)^4} \sum_{\sigma=\pm} \sigma e^{i\kappa_\sigma \pi} \int \tilde{\tau}^3 d \ln \tilde{\tau} W_{\kappa_\sigma, \mu_\alpha}^* (-2i\tilde{\tau}) W_{\kappa_\sigma, \mu_\alpha} (-2i\tilde{\tau}), \quad (3.43)$$

with $\kappa_\pm = \mp i\xi$ and $\mu_\alpha^2 = \frac{1}{4} - \frac{m_\alpha^2}{H^2}$. Therefore the baryon number density is given as

$$n_B \simeq -\frac{1}{3} g_R^2 H^3 [2\mathcal{K}(\xi, m_{W_R}) + \mathcal{K}(\xi, m_{Z_R})]. \quad (3.44)$$

The prefactor $\mathcal{K}(\xi, m_\alpha)$ with respect to ξ and m_{W_R} is shown in the left and right panels of Fig. 5. It increases (decreases) with the increase of ξ (m_α) and for $\xi > m_\alpha$ is

$$\mathcal{K}(\xi, m_\alpha) \propto \frac{1}{(2\pi)^4} e^{2\xi\pi}. \quad (3.45)$$

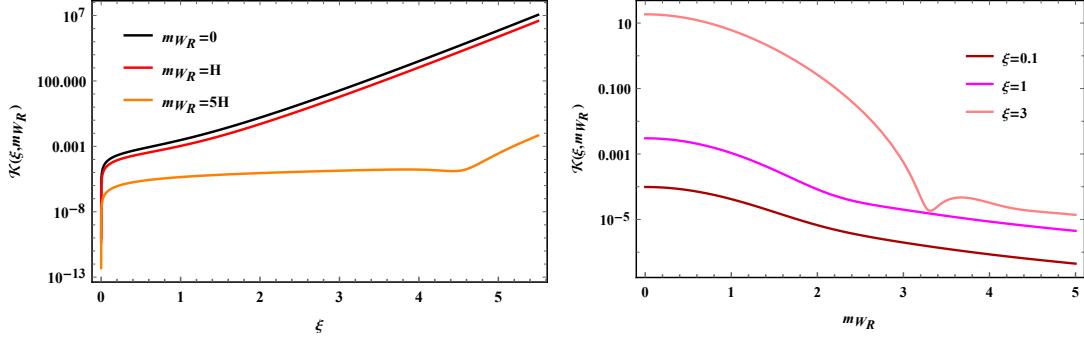


Figure 5. The factor $\mathcal{K}(\xi, m_{W_R})$ vs ξ (left panel) and vs m_{W_R} (right panel).

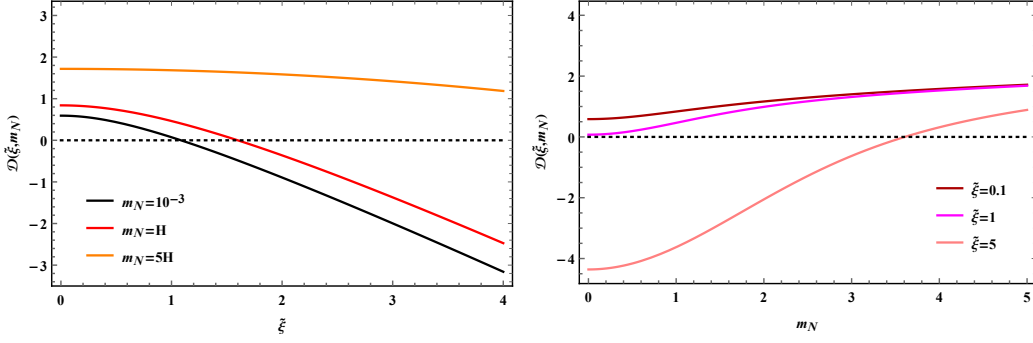


Figure 6. The prefactor $\mathcal{D}(\tilde{\xi}, m_{N_i})$ vs ξ (left panel) and vs m_{N_i} (right panel).

Due to the mass of the sterile neutrinos, the calculation of the lepton number is more involved and requires the mode functions. The leptonic field equations are

$$(i\sigma^\mu \partial_\mu + \frac{3i}{2}H + g_R \sigma^\mu \mathbf{W}_{R\mu} - \frac{\tilde{\lambda}\dot{\varphi}}{f})l_{iR} - m_{N_i} \nu_{iR}^c = 0, \quad (3.46)$$

$$\bar{n}_{N_i} \equiv \int d^3k \langle \nu_{iR}^\dagger \nu_{iR} \rangle = -H^3 \sum_i \frac{\tilde{\xi}}{\pi} \left(\frac{m_{N_i}}{H} \right)^2 \mathcal{D}(\tilde{\xi}, m_{N_i}), \quad (3.47)$$

where the bar emphasises that, unlike chiral anomaly, it is a classical effect. Using the point-splitting regularization, we computed $\nu_{i,R}$ and $\mathcal{D}(\tilde{\xi}, m_{N_i})$ analytically in App. B. The exact form of $\mathcal{D}(\tilde{\xi}, m_{N_i})$ is presented in Eq. (B.12) and we show it in Fig. 6. Here we discuss its qualitative behavior which in the large and small mass limits is

$$\mathcal{D}(\tilde{\xi}, m_{N_i}) \simeq \begin{cases} \frac{2}{\pi} \left[\ln \left(\frac{m_{N_i}}{H} \right) - \psi^{(0)}(1) + \frac{1}{2} \right] & \text{for } \frac{m_{N_i}}{H} \gg 1, \\ -\frac{4}{3}|\tilde{\xi}| & \text{for } \frac{m_{N_i}}{H} \ll 1. \end{cases} \quad (3.48)$$

The \bar{n}_{N_i} is directly proportional to (and an odd function of) $\tilde{\xi}$ which is the (classical) source of particle production. Moreover, it increases with the mass of the sterile neutrinos,

m_{N_i} , which is the cause of their chiral symmetry breaking in inflation. Therefore, the total number density of RHNs are given as

$$n_{N_i} = \bar{n}_{N_i} - \frac{1}{6} H^3 g_R^2 \left[\frac{2}{3} \mathcal{K}(\xi, m_{W_R}) + \frac{1}{3} \mathcal{K}(\xi, m_{Z_R}) \right]. \quad (3.49)$$

The final total lepton number is

$$n_L \simeq - \left[\frac{g_R^2}{3} [2\mathcal{K}(\xi, m_{W_R}) + \mathcal{K}(\xi, m_{Z_R})] + \sum_i \frac{\tilde{\xi}}{\pi} \left(\frac{m_{N_i}}{H} \right)^2 \mathcal{D}(\tilde{\xi}, m_{N_i}) \right] H^3. \quad (3.50)$$

3.3 Baryon and Lepton Numbers

Here we summarize the main features of inflationary baryon and lepton generation.

- The transverse modes of \mathbf{W}_R are generated by the axion that subsequently sources right-handed baryons and leptons.
- All the Sakharov conditions required for BAU are satisfied in inflation: i) Out of thermal equilibrium condition holds during inflation, ii) C is violated by the chiral nature of the $SU(2)_R$ interaction, iii) B , L , and CP are violated by the non-perturbative effects of \mathbf{W}_R .
- n_B and n_L are the total baryon and lepton number densities respectively. n_B and $n_{L_{SM}}$ are the contributions of the SM fermions. The RHNs number density is $n_N = n_L - n_{L_{SM}}$.
- The $B-L$ is conserved (violated) in scenario type-I (type-II). However, $B-L_{SM} = L_N$ is violated in both scenarios.
- In scenario type-I, the baryon and lepton numbers are both generated by the chiral anomaly of \mathbf{W}_R in inflation, i.e. $n_B = n_L \simeq -\frac{3g_R^2}{8\pi^2} n_{CS}$ (Eq. (3.24)). It can be written as

$$n_B = \alpha_{\text{inf}}(\xi) H^3, \quad (3.51)$$

where $\alpha_{\text{inf}}(\xi)$ is given as (see Fig. 7)

$$\alpha_{\text{inf}}(\xi) \simeq -g_R^2 \mathcal{K}(\xi). \quad (3.52)$$

- In scenario type-II, the baryon number is specified entirely by the chiral anomaly of \mathbf{W}_R , i.e. $n_B \simeq -\frac{3g_R^2}{8\pi^2} n_{CS}$ (Eq. (3.44)). In the leptonic sector, however, the massive RHNs are also generated by the axion. Therefore, the total lepton number is $n_L \simeq n_B + \bar{n}_N$ where \bar{n}_N is the RHNs produced by the axion (Eq. (3.47)).
- The number density of the RHNs generated in inflation is

$$n_{N_i} = \frac{1}{3} \tilde{\alpha}_{\text{inf}}(\xi, m_{N_i}) H^3, \quad (3.53)$$

where α_{inf} for scenarios type-I (Eq. (3.25)) and II (Eq. (3.49)) are given as

$$\tilde{\alpha}_{\text{inf}}(\xi, m_{N_i}) \simeq \begin{cases} -\frac{1}{2}g_R^2\mathcal{K}(\xi) & \text{Type-I,} \\ -\left(\frac{1}{2}g_R^2\left[\frac{2}{3}\mathcal{K}(\xi, m_{W_R}) + \frac{1}{3}\mathcal{K}(\xi, m_{W_Z})\right] + \frac{3\tilde{\xi}}{\pi}\left(\frac{m_{N_i}}{H}\right)^2\mathcal{D}(\tilde{\xi}, m_{N_i})\right) & \text{Type-II.} \end{cases} \quad (3.54)$$

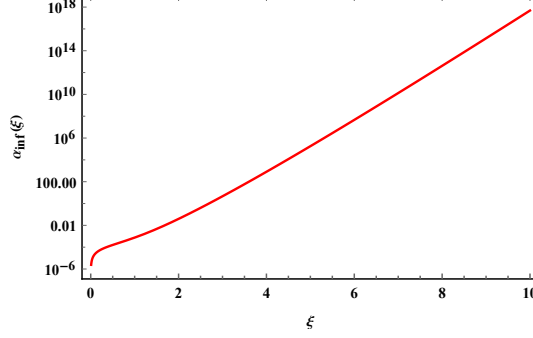


Figure 7. The $\alpha_{\text{inf}}(\xi)$ vs ξ in Eq. (3.52).

4 Post Reheating Evolution

To study the post-inflationary evolution, we need to specify our parameter space. For the sake of concreteness, we restrict the current analysis by assuming the following conditions considered by the author in [1]: **Condition C1)** A hierarchical mass spectrum for the RH neutrinos (as implied by the neutrino oscillations) as

$$m_{N_3} \gtrsim 10^{12} \text{ GeV} \gg m_{N_2} \gtrsim 10^9 \text{ GeV} \gg m_{N_1}, \quad (4.1)$$

where N_1 is much lighter than the EW scale with feeble Yukawa interactions and hence a DM candidate. (See Fig. 8) **Condition C2)** The W_R field is never in thermal equilibrium with the thermal bath, i.e. $T_{W_R} > T_{\text{reh}}$. **Condition C3)** The CP-violating phases in the neutrino sector, unconstrained by the current data, are not large enough to create the observed BAU. Reference [1] introduces a stronger version of the above conditions by imposing a more restrictive version of C2. **Restricted condition C2)** The post-inflationary generation of RHNs via W_R interactions is negligible compared to their pre-existing relics. We discuss and quantify conditions C2 & restricted C2 in Sec. 4.1 and condition C3 in Sec. 4.2.

4.1 Thermal Evolution

Reheating starts at some point after the end of inflation and ends at the formation of a dominant thermal bath with temperature T_{reh} . Here, we consider the phenomenological reheating model below

$$\rho_{\text{reh}} = \delta_{\text{reh}} \left(\frac{a_{\text{inf}}}{a_{\text{reh}}} \right)^4 \rho_{\text{inf}}, \quad (4.2)$$

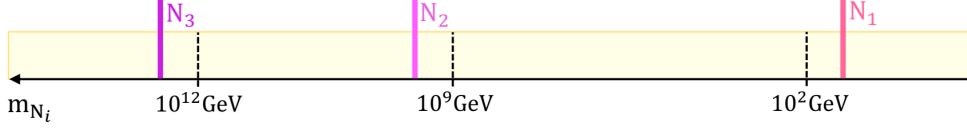


Figure 8. For concreteness we assume this hierarchical mass spectrum for right-handed neutrinos. The mass of N_1 is specified by the relic density of DM in Sec. 5.2.

in which ρ_{inf} and ρ_{reh} are the energy density at the end of inflation and reheating respectively. Moreover, δ_{reh} is the efficiency of the reheating process given as (See App. C.1)

$$\delta_{\text{reh}} \approx \exp[-(3w_X - 1)\Delta N], \quad \Delta N \equiv \ln\left(\frac{a_{\text{reh}}}{a_{\text{inf}}}\right), \quad (4.3)$$

where w_X is the effective equation of state in the intermediate period between the end of inflation and the formation of the thermal bath. The radiation energy density is given by

$$\rho_{\text{rad}}(T) = \frac{\pi^2}{30} g_{\text{eff}} T^4, \quad (4.4)$$

where g_{eff} is the effective number of relativistic degrees of freedom. For SM particles at the time of reheating we have $g_{\text{eff}} = 427/4$. The reheating temperature is

$$\frac{T_{\text{reh}}}{M_{\text{Pl}}} \approx \left(\frac{90}{g_{\text{eff}}}\right)^{\frac{1}{4}} \left(\frac{1}{\pi} \frac{H}{M_{\text{Pl}}}\right)^{\frac{1}{2}} \exp\left[-\frac{3(w_X + 1)}{4} \Delta N\right]. \quad (4.5)$$

The photon number density at the time of reheating is

$$n_{\gamma, \text{reh}} = \frac{2\zeta(3)}{\pi^2} T_{\text{reh}}^3, \quad (4.6)$$

where $\zeta(x)$ is the Riemann zeta function and $\zeta(3) \simeq 1.2$. The photon number density today is related to $n_{\gamma, \text{reh}}$ as

$$n_{\gamma, 0} = S n_{\gamma, \text{reh}} \left(\frac{a_{\text{reh}}}{a_0}\right)^3 \quad (4.7)$$

where S is the entropy injection factor. It captures the increase of entropy by the out of thermal equilibrium decay of heavy RHNs, and is worked out in App. C.1. We found that the entropy injection is negligible in our setup, i.e. ⁹

$$S \simeq 1. \quad (4.8)$$

▷ Condition C2:

The \mathbf{W}_R gauge interaction has essential effects on thermal properties of our setup. After

⁹Contrary to our setup, the late decay of long-lived $\mathbf{N}_{2,3}$ (with lifetime up to a second) which are produced via *freeze-out* mechanism can generate a sizable amount of entropy in the LRSM [44]. That requires a reheat temperature as low as a few *MeV* and $\mathbf{N}_{2,3}$ masses in the 100 *MeV* range.

the 1st SSB, they keep sterile neutrinos in thermal equilibrium by scattering with the SM fermions. The temperature of the freeze-out of \mathbf{W}_R gauge field can be estimated as

$$T_{W_R} \sim g_*^{\frac{1}{6}} \left(\frac{m_{W_R}}{10^{14} \text{GeV}} \right)^{\frac{4}{3}} \times 10^{13} \text{ GeV}, \quad (4.9)$$

where g_* is the number of relativistic degrees of freedom at T_{W_R} and m_{W_R} is the mass of W_R^\pm . The particles which are only coupled through the \mathbf{W}_R interactions with the thermal bath, e.g. \mathbf{N}_1 , gets decoupled at this point. The thermal evolution after inflation depends on whether sterile neutrinos are in thermal equilibrium initially or not. If in thermal equilibrium, \mathbf{W}_R interactions generate thermal abundances of RHNs, i.e., freeze-out production. The focus of this work, however, is the region in the parameter space in which \mathbf{W}_R interactions are never in thermal equilibrium, i.e. $T_{\text{reh}} < T_{W_R}$ which demands (See Fig. 9)

$$\frac{H}{M_{\text{Pl}}} \lesssim \frac{3}{2} \times 10^{-9} \exp \left[\frac{3(w_X + 1)}{2} \Delta N \right] \left(\frac{g_{\text{eff}}}{10^2} \right)^{\frac{1}{2}} \left(\frac{g_*}{10^2} \right)^{\frac{1}{3}} \left(\frac{m_{W_R}}{10^{14} \text{GeV}} \right)^{\frac{8}{3}}. \quad (4.10)$$

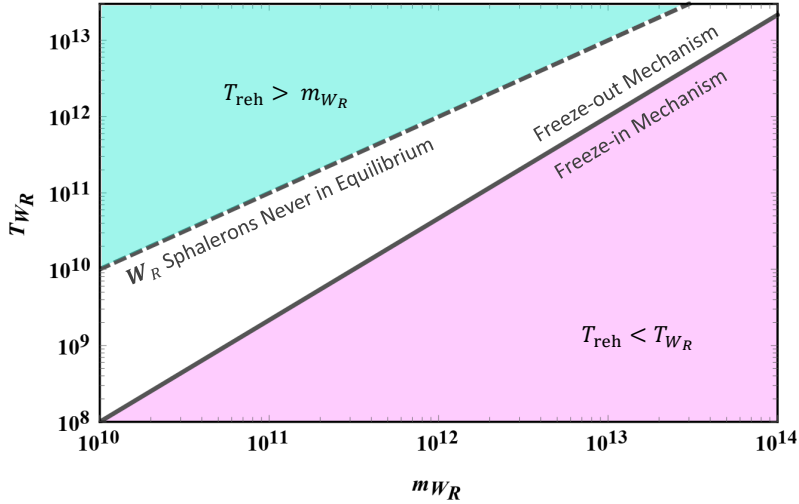


Figure 9. The freeze-out temperature of \mathbf{W}_R interactions in terms of m_{W_R} . The (pink) shaded area shows regions with $T_{\text{reh}} < T_{W_R}$ (condition C2) and below the solid line, the secondary (post-inflationary) abundance of RHNs are not generated by freeze-out but instead by the freeze-in mechanism. In the (blue) shaded region we have $T_{\text{reh}} > m_{W_R}$, so \mathbf{W}_R sphalerons are never in thermal equilibrium below the dashed line.

The above condition guarantees that \mathbf{N}_i does not have thermal abundances by freeze-out mechanism.¹⁰ However, as we will see shortly, \mathbf{W}_R scatterings may still create a post inflationary abundance of RHNs via freeze-in mechanism. Fig. 9 presents T_{W_R} vs m_{W_R} and the (pink) shaded area shows the region with $T_{\text{reh}} < T_{W_R}$ which is the focus of the

¹⁰In case that $T_{W_R} < T_{\text{reh}}$, Fermi-type theory of \mathbf{W}_R field keeps sterile neutrinos in thermal equilibrium even at temperatures lower than m_{W_R} . The freeze-out relic abundance of \mathbf{N}_i is $\frac{n_{N_i}}{s} = \frac{135\zeta(3)}{4\pi^4} \frac{1}{g_*(T_{W_R})}$.

current work. The (blue) shaded region marks where $T_{\text{reh}} > m_{W_R}$. Therefore, in the region of our interest the $SU(2)_R$ sphalerons are never in thermal equilibrium to cause any B + L violating interaction (see Eq. (D.5)). That is in contrast to the $SU(2)_L$ sphalerons which are in thermal equilibrium in the wide temperature interval of $m_{W_L} < T < 10^{12} \text{ GeV}$. Another constraint on Hubble parameter in inflation comes from the current upper bound on the tensor to scalar ratio, $r_{0.05} < 0.07$ at 95% confidence [45], which implies $H \lesssim 10^{-5} M_{\text{Pl}}$.

▷ **Restricted Condition C2:**

At reheating, the pre-existing RHNs, generated in inflation, is Eq. (3.54)

$$n_{N_i}^p \approx \frac{1}{3} \alpha_{\text{inf}}(\xi) \exp[-3\Delta N] H^3. \quad (4.11)$$

One of the consequences of condition C2 is that the RHN does not have a thermal abundance, i.e. no freeze-out production. However, post-inflationary \mathbf{W}_R scatterings produce RHNs via freeze-in as [46]

$$n_{N_i}^s \approx 10^{13} \times \left(\frac{g_{\text{eff}}}{10^2} \right) \left(\frac{T_{\text{reh}}}{M_{\text{Pl}}} \right)^6 \left(\frac{10^{14} \text{ GeV}}{m_{W_R}} \right)^4 M_{\text{Pl}}^3. \quad (4.12)$$

The superscripts p in Eq. (4.11) and s in Eq. (4.12) denote contributions of pre-existing (inflationary) and secondary (freeze-in) production respectively. One can restrict condition C2 such that this secondary RHN production is subleading comparing to the pre-existing one. Using Eq. (4.5), we can quantify restricted condition C2 as

$$\frac{n_{N_i}^s}{n_{N_i}^p} \approx \frac{8 \times 10^{11}}{\alpha_{\text{inf}}(\xi)} \exp \left[-\frac{3}{2} (1 + 3w_X) \Delta N \right] \left(\frac{10^2}{g_{\text{eff}}} \right)^{\frac{1}{2}} \left(\frac{10^{14} \text{ GeV}}{m_{W_R}} \right)^4 < 1, \quad (4.13)$$

once inequality in Eq. (4.10) holds.

Type-I Scenarios: In this case, the \mathbf{W}_R gauge fields and N_i s are massless in inflation. On the other hand, condition C2 demands $m_{W_R} \gtrsim T_{\text{reh}}$ which implies the first SSB must happen shortly after the end of inflation.

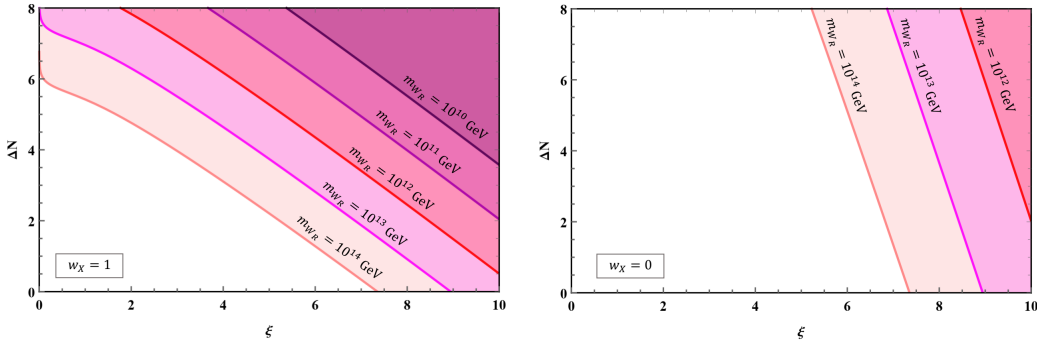


Figure 10. Condition restricted C2 in type-I scenarios. The shaded area above each line corresponds to the accessible parameter space for a given m_{W_R} that satisfies Eq. (4.13). The left and right panels show $w_X = 1$ and $w_X = 0$ respectively. The Max of m_{W_R} is set to be 10^{-2} GUT scale.

The shaded areas in Fig. 10 show the parameter space in which restricted C2 is satisfied for a given m_{W_R} . As we see, most of the parameter space is accessible in case of $w_X = 1$ while the case with $w_X = 0$ requires larger values of m_{W_R} and ΔN and/or ξ . The ratio of the pre-existing N_1 to its freeze-in production in type-I can be analytically approximated as

$$\frac{n_{N_i}^s}{n_{N_i}^p} \sim 10^{11} \exp \left[-\frac{3}{2}(1 + 3w_X)\Delta N - 2\pi\xi \right] \left(\frac{10^{14} \text{GeV}}{m_{W_R}} \right)^4. \quad (4.14)$$

Type-II Scenarios: In this case the $SU(2)_R$ gauge fields and N_i s are massive in inflation. However, N_1 which is the dark matter candidate is very light compared to H . Therefore, the pre-existing N_1 in Eq. (4.13) is produced by the chiral anomaly in inflation. The mass of the W_R can be roughly estimated as $m_{W_R} \sim \sqrt{\frac{H}{M_{\text{Pl}}}} M_{\text{Pl}}$. For $m_{W_R} = 10^2 H$, Fig. 11 shows the parameter space corresponding to each ξ in which restricted C2 is satisfied. Comparing with the type-I scenario, the C2 is satisfied in a smaller part of the parameter space and only for $w_X = 1$ case.

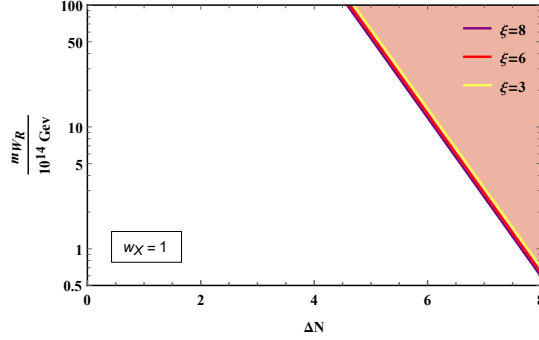


Figure 11. The parameter space $(\Delta N, m_{W_R})$ for different values of ξ that satisfies condition restricted C2 in type-II scenarios with $w_X = 1$. The accessible region for $w_X = 0$ case is in the region with $\Delta N > 8$ and it is not shown here.

To summarize, condition restricted C2 prefers type-I scenarios and $w_X = 1$. In particular, it holds in a wide part of the parameter space when $\Lambda_F \lesssim \Lambda_{\text{inf}}$, i.e., the first SSB coincides with the end of inflation. Interestingly, it relates left-right gauge symmetry breaking to a geometrical phase transition in cosmology, i.e., the end of exponential expansion of the Universe. Moreover, as Figs. 10-11 show, it demands $m_{W_R} > 10^{10} \text{ GeV}$ which is the scale suggested by the non-supersymmetric $SO(10)$ GUT model with an intermediate left-right symmetry scale [47–49].

4.2 Spectator Effects, RHN decay, and Matter Asymmetry

Throughout the Early Universe, particles experience a whole cascade of interactions that eventually equilibrate in the Early Universe. Many of them can potentially redistribute the initial asymmetries to the spectator degrees of freedom. These processes do not participate directly in the generation or washout of the asymmetries (hence the name spectator). Still, they have important effects in final B and L by imposing certain relations between different

species. In addition to the spectator effects, the CP asymmetric decay of $\mathbf{N}_{2,3}$ produces SM leptons and simultaneously partially washes out the pre-existing lepton asymmetries. In this section, we consider washout effects, lepton flavor effects, and sphaleron processes. For the ease of notation, we denote the SM leptons as $\underline{\mathbf{L}}$, i.e.

$$\underline{\mathbf{L}} \equiv \mathbf{L}_{\text{SM}}. \quad (4.15)$$

Spectator Effects

The $SU(2)_L$ sphalerons ($SU(2)_R$ sphalerons) transmit the asymmetry from left-handed (right-handed) leptons to left-handed (right-handed) quarks and vice versa. The \mathbf{W}_L gauge field is inactive and unimportant in inflation. Later on, however, they attain a thermal equilibrium, and together with \mathbf{W}_R , they can have significant impacts on the final \mathbf{B} and \mathbf{L} asymmetries. The $\mathbf{B} + \mathbf{L}$ violating processes due to $W_{L,R}$ sphalerons shuffle the initial baryons and leptons coupled to them. In App. D.1 we showed that W_R sphalerons are never in thermal equilibrium in our setup (see also Fig. 9). Hence they can not give rise to $\mathbf{B} + \mathbf{L}$ violating processes. After the \mathbf{W}_R and sterile neutrinos' freezeout, the SM particles remain in thermal equilibrium up to the electroweak scale. Quarks, SM leptons, and Higgs bosons interact via gauge and Yukawa interactions as well as non-perturbative sphaleron processes. All the SM gauge interactions and W_L sphaleron processes are in equilibrium in the temperature range of $100 \text{ GeV} \lesssim T \lesssim 10^{12} \text{ GeV}$. The thermal equilibrium of Yukawa interactions is flavor-dependent. Nevertheless, all of them are in equilibrium at $T < 85 \text{ TeV}$ [50]. Using the sphaleron effects and hypercharge constraint, we find that \mathbf{B} , $\underline{\mathbf{L}}$, and $\mathbf{B} - \underline{\mathbf{L}}$ are related as

$$n_{\mathbf{B}} = c_{\text{sph}} n_{\mathbf{B}-\underline{\mathbf{L}}}, \quad (4.16)$$

$$n_{\underline{\mathbf{L}}} = (c_{\text{sph}} - 1) n_{\mathbf{B}-\underline{\mathbf{L}}}. \quad (4.17)$$

where $c_{\text{sph}} = \frac{28}{79}$ is the sphaleron conversion factor.

Lepton Flavor Effects

One potentially very significant aspect of (post inflationary) leptogenesis is the flavor effect. The flavor-dependent washout and \mathbf{L} violating interactions can significantly change the value, and even sign of the final baryon asymmetry [51–53]. By the end of inflation, and due to our flavor blind CP violating source, we have a lepton quantum state $|l_{\text{inf}}\rangle$ as

$$|l_{\text{inf}}\rangle \equiv \sum_{\alpha=e,\mu,\tau} C_{\alpha}^{\text{inf}} |\alpha\rangle \quad \text{where} \quad C_{\alpha}^{\text{inf}} = \langle \alpha | l_{\text{inf}} \rangle. \quad (4.18)$$

The decays of the heavy sterile neutrinos modify these initial states. More precisely, the CP asymmetric decay of \mathbf{N}_i produces leptons as ¹¹

$$|l_i\rangle \equiv \sum_{\alpha=e,\mu,\tau} C_{i\alpha} |\alpha\rangle \quad \text{where} \quad C_{i\alpha} = \langle \alpha | l_i \rangle, \quad (4.19)$$

¹¹The $C_{i\alpha}$ coefficients are given by the Yukawa matrix. In terms of the active neutrino mass matrix we have $C_{i\alpha} = \frac{m_{\nu}^{\alpha i}}{\sqrt{(m_{\nu}^{\dagger} m_{\nu})_{\alpha\alpha}}}$. Unlike $|\alpha\rangle$ s, $|l_i\rangle$ does not form an orthonormal bases, i.e. in general $\langle l_i | l_j \rangle \neq \delta_{ij}$.

and simultaneously washes out the pre-existing (inflationary) leptons in this direction, i.e.

$$|l_{inf}\rangle_i \equiv \langle l_i | l_{inf} \rangle |l_i\rangle. \quad (4.20)$$

However, the pre-existing leptons normal to $|l_i\rangle$ direction, i.e.

$$|l_{inf}\rangle_i^\perp \equiv |l_{inf}\rangle - |l_{inf}\rangle_i, \quad (4.21)$$

elude the washout. As discussed earlier, we assume that \mathbf{N}_1 has feeble Yukawa interactions with the SM and hence a DM candidate (condition C1). Therefore, only \mathbf{N}_2 and \mathbf{N}_3 contribute to the seesaw mechanism as well as decays and washouts. As a result, the component $|l_{inf}\rangle_{3\perp 2\perp}$ which is normal to both $|l_3\rangle$ and $|l_2\rangle$ remains as the remnant of the initial asymmetry. For the mass spectrum in Eq. (4.1), the corresponding Boltzmann equations and details are presented in App. D.2 and here we report the final results. The geometry of this process in the SM flavor basis is schematically shown in Fig. 12.

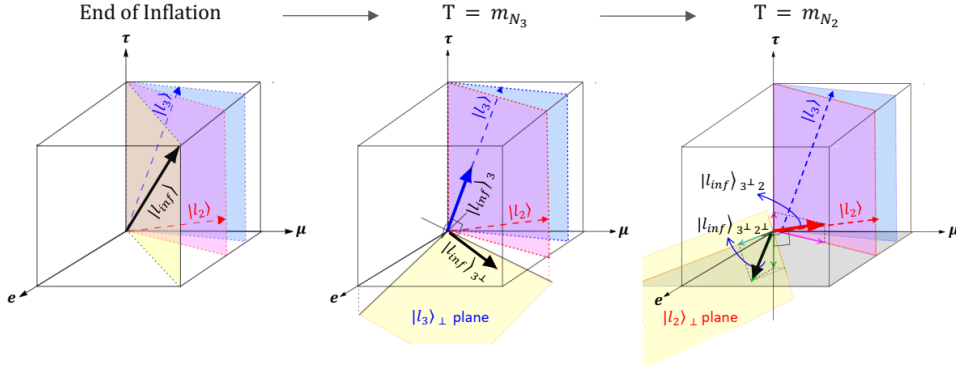


Figure 12. The geometrical illustration of washout processes induced by the decay of \mathbf{N}_3 and \mathbf{N}_2 . The left panel shows the SM leptonic states at the end of inflation $|l_{inf}\rangle$ in black and $|l_{3,2}\rangle$ in blue and red, respectively. The middle panel shows the SM lepton states at $T = m_{N_3}$ and the right panel presents the system at $T = m_{N_2}$. The black arrows in each panel show the pre-existing SM lepton asymmetry, which remains untouched by the washout effects. (Fig. adopted from ref. [1])

▷ **Condition C3:**

The SM lepton asymmetry after decay of \mathbf{N}_2 at $T = M_2 \gtrsim 10^9 \text{ GeV}$ is

$$n_{\mathbf{B}-\mathbf{L}} = n_{\mathbf{B}-\mathbf{L}}^{p,f} + n_{\mathbf{B}-\mathbf{L}}^{\mathbf{N}}, \quad (4.22)$$

where $n_{\mathbf{B}-\mathbf{L}}^{p,f}$ is the remnant of the primordial asymmetry $n_{\mathbf{B}-\mathbf{L}}^{p,i}$, and $n_{\mathbf{B}-\mathbf{L}}^{\mathbf{N}}$ is the lepton number produced by the CP asymmetric decay of \mathbf{N}_2 as

$$n_{\mathbf{B}-\mathbf{L}}^{\mathbf{N}} \approx \varepsilon_2 \kappa_2, \quad (4.23)$$

where ε_2 is the CP asymmetry and κ_2 is the associated efficiency factor. Interestingly, when flavour effects are considered, it is very difficult for the pre-existing asymmetry to be washed out by the RH neutrinos [54, 55]. The value of $n_{\mathbf{B}-\mathbf{L}}^{\mathbf{N}}$ depends on the leptonic Yukawa matrix and the unconstrained CP violating phases in the neutrino sector. In this

work, we assume that the amount of this asymmetry is not sufficient to account for the observed matter asymmetry, i.e. condition C3:

$$\frac{n_{\mathbf{B}-\underline{\mathbf{L}}}^{\mathbf{N}}}{n_{\mathbf{B}-\underline{\mathbf{L}}}^{p,f}} \ll 1. \quad (4.24)$$

Condition C3 is the opposite limit of what is assumed in leptogenesis scenarios [56].

Finally the remnant of the primordial asymmetry is given as below in terms of the initial $\mathbf{B} - \underline{\mathbf{L}}$

$$n_{\mathbf{B}-\underline{\mathbf{L}}} \simeq n_{\mathbf{B}-\underline{\mathbf{L}}}^{p,f} = \mathcal{C} n_{\mathbf{B}-\underline{\mathbf{L}}}^{p,i}, \quad (4.25)$$

where \mathcal{C} is a parameter less than one (see Eq. (D.35) and Fig. 15). For most of the parameter space we have

$$\mathcal{C} \gtrsim \frac{1}{3}. \quad (4.26)$$

Eliminating the effect of this pre-existing asymmetry is very hard and requires tightly fine-tuned relations between leptonic Yukawa couplings and the physics of inflation which is discussed in App D.2.

5 Modern Era Baryon Asymmetry and Dark Matter

In this section we work out the baryon to photon ratio and dark matter density today. Here we only consider type-I scenarios in which the 1st SSB happens after inflation. The remnants of the inflationary baryon and SM lepton asymmetries after the decay of the heavy RHNs and the getting redistributed by the spectator effects are respectively as

$$n_{\mathbf{B}}(a) \simeq 0.12 \alpha_{\text{inf}}(\xi) H^3 \exp[-3\Delta N] \left(\frac{a_{\text{reh}}}{a} \right)^3, \quad (5.1)$$

$$n_{\mathbf{L}_{\text{SM}}}(a) \simeq -0.18 n_{\mathbf{B}}(a). \quad (5.2)$$

The final \mathbf{N}_1 number density is

$$n_{\mathbf{N}_1}(a) \simeq 2.8 n_{\mathbf{B}}(a) + n_{\mathbf{N}_1}^s(a), \quad (5.3)$$

where $n_{\mathbf{N}_1}^s$ is the secondary (freeze-in) production of \mathbf{N}_1 given in Eq. (4.12). As is assumed in [1], if the restricted version of condition C2 in Eq. (4.13) holds, we have

$$n_{\mathbf{N}_1}(a) \simeq 2.8 n_{\mathbf{B}}(a). \quad (5.4)$$

The particle production mechanism throughout cosmic evolution is then summarized in Fig. 2.

5.1 Baryon to Photon Ratio

To the best of our knowledge, the cosmos is highly matter-dominated. The baryon-antibaryon asymmetry can be quantified by the baryon to photon ratio at the present time as [57]

$$\eta_{\text{B}}^0 = \frac{n_{\text{B}}^0}{n_{\gamma}^0} \simeq 6 \times 10^{-10}, \quad (5.5)$$

in which a 0 superscript denotes the present time value. Our setup predicts the baryon to photon ratio as

$$\eta_{\text{B}}^0 \approx 3 \left(\frac{g_{\text{eff}}}{100} \right)^{\frac{3}{4}} \frac{\alpha_{\text{inf}}(\xi)}{(\delta_{\text{reh}})^{\frac{3}{4}}} \left(\frac{H}{M_{\text{Pl}}} \right)^{\frac{3}{2}}, \quad (5.6)$$

where $g_{\text{eff}} = 427/4$. One can write η_{B}^0 in terms of the curvature power spectrum as

$$\eta_{\text{B}}^0 \approx 0.3 \beta P_{\zeta}, \quad (5.7)$$

where $P_{\zeta}(k_0) = \frac{1}{2(2\pi)^2\epsilon} \left(\frac{H}{M_{\text{Pl}}} \right)^2$ in which ϵ is the slow-roll parameter, and β is

$$\beta = \frac{5 (4\pi)^2 \epsilon \alpha_{\text{inf}}(\xi)}{(\delta_{\text{reh}})^{\frac{3}{4}}} \left(\frac{M_{\text{Pl}}}{H} \right)^{\frac{1}{2}}. \quad (5.8)$$

To agree with the date, β should be one and we have

$$\frac{H}{M_{\text{Pl}}} \approx 10^{-6} \alpha_{\text{inf}}^{-\frac{2}{3}}(\xi) \delta_{\text{reh}}^{\frac{1}{2}}. \quad (5.9)$$

By this point, we have three constraints on H , i.e. Eq. (4.10) imposed by C2, Eq. (5.9) to explain the observed η_{B} , and the upper bound enforced by CMB data. Combining Eqs (4.10) and (5.9) gives

$$\alpha_{\text{inf}}^{\frac{2}{3}}(\xi) \delta_{\text{reh}}^{\left(\frac{1/3+w_X}{1/3-w_X}\right)} \left(\frac{m_{W_R}}{10^{14} \text{ GeV}} \right)^{\frac{8}{3}} \gtrsim 10^3, \quad (5.10)$$

which together with $\sqrt{H M_{\text{Pl}}} < 10^{15} \text{ GeV}$ specifies the accessible region of the parameter space. The color shaded areas (with solid line boundaries) in Fig. 13 show allowed parts of the parameter space for different values of m_{W_R} while the gray shaded area shows the region with $\sqrt{H M_{\text{Pl}}} < 10^{15} \text{ GeV}$. The boundaries of accessible parameters in the more restrictive case with condition restricted C2 in Eq. (4.13) are shown with same color (dashed lines) in Fig. 13. This setup can explain the observed η_{B} for typical values of the parameters and in a wide range of the parameter space. Interestingly, it prefers left-right symmetry breaking scales above 10^{10} GeV , which is in the range suggested by the non-supersymmetric SO(10) Grand Unified Theory with an intermediate left-right symmetry scale.

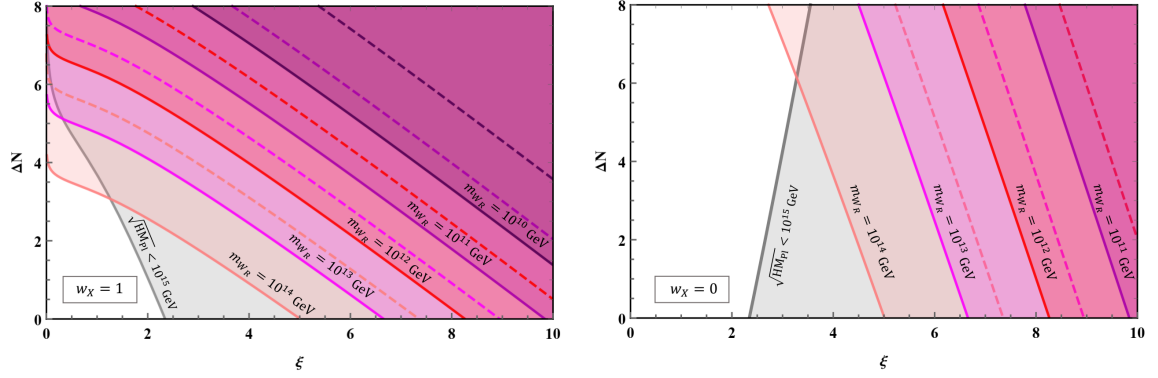


Figure 13. The accessible parameter space in terms of ξ , ΔN , and m_{W_R} for $w_X = 1$ (Left Panel) and $w_X = 0$ (Right Panel). The color shaded areas (with solid line boundaries) present regions that Eq. 5.10 is satisfied while the gray shaded region shows areas associated with $\sqrt{HM_{\text{Pl}}} < 10^{15} \text{ GeV}$. The dashed lines present the boundaries corresponding to the same colors but with restricted C2 condition.

5.2 Right-handed Neutrino as Cold Dark Matter

As discussed in Sec. 4, we assume that the lightest RHN, \mathbf{N}_1 , has feeble Yukawa couplings, hence decouples after freezeout of W_R interactions at T_{W_R} with a relic density given as

$$\Omega_{\mathbf{N}_1} \approx 2.8 \frac{m_{\mathbf{N}_1}}{m_p} \Omega_B \left(1 + \frac{n_{\mathbf{N}_1}^s}{n_p^p}\right), \quad (5.11)$$

where Ω_B is the baryon density parameter, m_p is the proton mass. If \mathbf{N}_1 makes all of the DM that we observe today, i.e. $\Omega_{\mathbf{N}_1} \simeq 5\Omega_B$, it specifies the mass of \mathbf{N}_1 in terms of the proton mass as

$$m_{\mathbf{N}_1} \approx \frac{1.8 m_p}{\left(1 + \frac{n_{\mathbf{N}_1}^s}{n_p^p}\right)}. \quad (5.12)$$

Condition C2 implies that $0 \leq \frac{n_{\mathbf{N}_1}^s}{n_p^p} < 10^6$ which specifies the mass of \mathbf{N}_1 in the wide range of a few keV to a few GeV . That mass range is associated to different DM spectra from warm DM to cold DM. On the other hand if following [1] we consider restricted condition C2 which guarantees that the \mathbf{N}_1 relic density is primordial, we have

$$\Omega_{\mathbf{N}_1} \approx 2.8 \frac{m_{\mathbf{N}_1}}{m_p} \Omega_B, \quad (5.13)$$

which makes a specific prediction for the mass of \mathbf{N}_1 as

$$m_{\mathbf{N}_1} \simeq 1.8 m_p = 1.7 \text{ GeV}. \quad (5.14)$$

That leads to a cold DM spectrum that is consistent with structure formation. Next, we study the stability of \mathbf{N}_1 as a DM particle.

Decay of \mathbf{N}_1

Given that W_R is very heavy and freezes out early (see Sec. 4.1), the dominant decay channel of \mathbf{N}_1 is $\mathbf{N}_1 \rightarrow 3\nu$ with the total decay width [58, 59]

$$\Gamma_{\mathbf{N}_1 \rightarrow 3\nu} = \frac{G_F^2 M_{\mathbf{N}_1}^5}{96 (2\pi)^3} \sum_{\alpha} \sin^2(2\theta_{\alpha,1}), \quad (5.15)$$

where G_F is the Fermi constant, $\alpha = e, \nu, \tau$ and $\theta_{\alpha,1}$ are the mixing angles of left-handed neutrinos with \mathbf{N}_1 . Demanding that the lifetime of this process, $t_{\mathbf{N}_1}$, is larger than the age of the Universe, i.e. $t_U \approx 4.4 \times 10^{17}$ s, we arrive at

$$\frac{t_{\mathbf{N}_1}}{t_U} \approx \left(\frac{0.56 \text{ GeV}}{M_{\mathbf{N}_1}} \right)^5 \left(\frac{10^{-26}}{\theta_1^2} \right), \quad (5.16)$$

where $\theta_1^2 \equiv \sum_{\alpha} \theta_{\alpha,1}^2$. Demanding that \mathbf{N}_1 is stable over the lifetime of the universe gives

$$\theta_1 < 10^{-13}. \quad (5.17)$$

In this framework, the generation mechanism of \mathbf{N}_1 is independent of its Yukawa mixing with active neutrinos, and θ_1 can be any number that satisfies the above upper bound. The next leading decay channel is the loop-mediated radiative decay of \mathbf{N}_1 to active neutrinos and a gamma-ray photon with energy $E_{\gamma} \approx M_{\mathbf{N}_1}/2$ as [58]

$$\Gamma_{\mathbf{N}_1 \rightarrow \gamma \nu} = \frac{9\alpha_{em} G_F^2 M_{\mathbf{N}_1}^5}{64 (2\pi)^4} \sum_{\alpha} \sin^2(2\theta_{\alpha,1}) \sim 10^{-2} \Gamma_{\mathbf{N}_1 \rightarrow 3\nu}. \quad (5.18)$$

Although the radiative decay has a branching ratio of order 2%, it can provide upper bounds from not observing gamma-ray photons with energy E_{γ} . The current strongest gamma-ray bounds in the GeV scale are on mass range 10-100 GeV [60] which is much heavier than our DM.

6 Quick on Observational Constraints and Signatures

In this section, we briefly discuss the cosmological, astrophysical, and collider constraints and signatures of our setup. The current work is based on embedding the minimal $SU(2)$ -axion inflation model [17] in minimal LRSM [2–4]. The cosmic perturbations of the minimal $SU(2)$ -axion inflation in the presence of the gauge field VEV has been studied and compared with Planck data in [17]. In the current work, however, we solely focus on scenarios with vanishing VEV. Hence it enjoys a wider accessible parameter space. As a cosmological smoking gun, all $SU(2)$ -axion inflation models predict chiral [18, 31, 32] and non-Gaussian [33] gravitational wave background which leads to parity odd CMB cross-spectra [35]. This chiral GW Background (GWB) is blue tilted and can also be detected by future laser interferometer detectors. The parity odd features can be used as an observational marker to distinguish it from the standard GWB produced by the vacuum fluctuations [61–63]. This signal has been extensively studied in the literature. For an exhaustive discussion on the measurement of this effect, see [34].

Direct production or virtual contributions at astrophysical and collider processes put several constraints on the charged and neutral $SU(2)_R$ gauge boson mass and mixing parameters. The $K_L - K_S$ kaon mass difference measurement [64] places a lower bound on the mass of W_R as $m_{W_R} > 1.6 \text{ TeV}$ and the mixing angle between Z_R and Z_L is constrained to be less than 10^{-4} . The possible low-energy W_R has been the target of several LHC collaborations which puts the current bound as $m_{W_R} > 3 \text{ TeV}$ [65]. For an exhaustive discussion of the phenomenological implications and constraints of LRSM, see [66]. Our current setup with high scale $SU(2)_R$ SSB, i.e., $m_{W_R} > 10^{10} \text{ GeV}$, satisfies the above lower bounds. The most distinctive astrophysical signal of our DM candidate with GeV mass is the gamma-ray line at $E = m_{N_1}/2$ produced in the one-loop decay $N_1 \rightarrow \gamma \nu$. Gamma-ray lines have been probed by the Fermi-LAT [60], H.E.S.S. [67], and MAGIC telescopes [68]. However, the strongest current bounds are on DM masses above 10 GeV [60] which is heavier than our DM. We leave the further study of the observable signatures of this setup for future work.

7 Conclusions

Recently [1] proposed a new particle physics model for inflation, based on embedding axion-inflation in gauge extensions of the SM. To unify cosmic inflation and BSM, it utilized the minimal Left-Right Symmetric Model (LRSM) [2–4] with gauge group $SU(2)_L \times SU(2)_R \times U(1)_{B-L}$. As the name implies, the model includes \mathbf{W}_R gauge bosons and three right-handed neutrinos (RHN). As the inflaton field, an axion is added to the field content of LRSM, which is directly coupled to the $SU(2)_R$ gauge field. In this work, we presented the analytical and numerical details of this setup.

LRSM in cosmology introduces a new fundamental cosmic scale, i.e., feeble scale Λ_F , where the extended gauge symmetry breaks down to the SM one, i.e., $SU(2)_R \times U(1)_{B-L} \rightarrow U(1)_Y$. At feeble scale, the W_R^\pm and Z_R^0 become massive, and the RHNs acquire Majorana masses [7]. Later, at the electroweak scale, the second spontaneous symmetry breaking happens, which gives mass to the SM particles. At this point, the left-handed neutrinos acquire mass by seesaw mechanism [7] (for cosmic evolution see Fig. 1). Based on the scale of inflation $\Lambda_{\text{inf}} = \sqrt{H M_{\text{Pl}}}$, feeble scale Λ_F , and the (possible) $SU(2)_R$ field's VEV in inflation, one can separate four different types of scenarios (see table 1). Following [1], we solely focused on scenarios with vanishing $SU(2)_R$ VEV, i.e. type-I ($\Lambda_{\text{inf}} > \Lambda_F$) & type-II ($\Lambda_{\text{inf}} < \Lambda_F$) scenarios.

The $SU(2)_R$ gauge field is produced by inflaton while other gauge fields, i.e., $SU(3)$, $SU(2)_L$ and $U(1)_{B-L}$, are diluted by the exponential expansion. The chiral anomaly of \mathbf{W}_R breaks CP in physics of inflation and gives rise to simultaneous baryogenesis, leptogenesis, and RHN creation in inflation (see Eq.s (3.24) & (3.25) for type-I and Eq.s (3.44) & (3.50) for type-II scenarios). Even in type-I scenarios in which $B - L$ is a gauge symmetry in inflation, we have $B - L_{\text{SM}} \neq 0$. For cosmic evolution after inflation, we future specified our parameters and imposed the three conditions which are used in [1]. Condition C1 considered a hierarchical mass spectrum for RHNs with feeble Yukawa interactions for N_1 such that it is a DM candidate (Eq. (4.1)). Condition C2 demands that \mathbf{W}_R is never in thermal equilibrium with the thermal bath. Consequently, it implies; 1) the $SU(2)_R$

sphalerons were never in equilibrium as well (Eq. (4.10) and Fig. 9), and 2) there is no secondary freeze-out production of RHNs. However, the post-inflationary scatterings of W_R can generate RHNs via freeze-in mechanism (Eq. (4.12)). Following [1], one can also consider a restricted version of condition C2 which demands that this secondary RHN production is subleading comparing to the pre-existing one (Eq. (4.13)). Finally, condition C3 assumed that the unconstrained CP-violating phases in the neutrino sector are not strong enough to make a sizable contribution to the matter asymmetry (Eq. (4.24)). C3 is the opposite limit of what is assumed in leptogenesis scenarios.

The lightest RHN gets decoupled after the freeze-out of W_R field at T_{W_R} (Eq. (4.9)). The heavier RHNs decay after temperature gets below their masses, and the spectator effects reshuffle the primordial baryon and SM lepton numbers. The final baryon to photon ratio and DM relic density are presented in Eqs (5.6) and (5.11) respectively. This setup can explain η_B and Ω_{DM} in a wide range of its parameter space (see Fig. 13). If N_1 makes all the DM relic density, then its mass is in the range of $keV - GeV$. In case that restricted C2 condition holds, the mass is predicted to be $m_{N_1} \approx 1.7 GeV$, i.e. a cold DM spectra consistent with structure formation (Eq. (5.14)). In that case, baryogenesis and DM today are the remnants of a pure quantum effect (chiral anomaly of W_R) in inflation. Consequently, it can naturally explain the observed coincidences among cosmological parameters, i.e., $\eta_B = 0.3P_\zeta$ and $\Omega_{DM} = 5\Omega_B$. Besides, this model is a complete setup that can simultaneously provide plausible explanations for the phenomena (I-IV) named in the introduction. The summary of this new mechanism is illustrated in Fig. 2.

It is noteworthy to mention that we can couple the axion to both $SU(2)_R$ and $SU(2)_L$ gauge fields. However, the inflationary production of left-handed baryons and leptons by $SU(2)_L$ (i.e. $B_{SM} = L_{SM}$) will be completely washed out by the $SU(2)_L$ sphaleon effects which are in thermal equilibrium between T_{reh} and m_{W_L} . Since $SU(2)_L$ -axion interaction leaves no fermionic remnants today, it is neglected in the minimal realization of this idea proposed in [1].

In this setup, P and CP are broken by the VEV of the axion and its interaction with the gauge field. It provides a deep connection between inflation, matter asymmetry, and DM relic density. This alternative mechanism, therefore, does not rely on the largeness of the unconstrained CP-violating phases in the neutrino sector nor fine-tuned masses for the heaviest right-handed neutrinos. Interestingly, sufficient matter creation relates the feeble scale to a geometrical phase transition in cosmology, i.e., the end of exponential expansion of the Universe. Moreover, it demands $m_{W_R} > 10^{10} GeV$ (see Figs 10-11) which is the scale suggested by the non-supersymmetric SO(10) GUT model with an intermediate left-right symmetry scale [47–49]. The above relations between the energy scales may be hints of a fundamental connection that we leave for future work. As yet another added benefit, this setup comes with a cosmological smoking gun; chiral, non-Gaussian, and blue-tilted gravitational wave background, which can be probed by future CMB missions and laser interferometer detectors. For an exhaustive discussion on the measurement of this effect, see [34].

Acknowledgments

The author especially thanks Eiichiro Komatsu for insightful discussions and valuable input during previous collaborations. She also likes to thank G. Giudice, J. Kopp, and M. Shaposhnikov for valuable discussions.

A Overview of Minimal Left-Right Symmetric Theories

Here we review the aspects of minimal left-right symmetric models (LRSM) [2–5] that we need in this paper.

Field and Matter Content:

The model’s field content is presented in Table 2, and in the following, we explain the gauge field, extended Higgs, and fermionic sectors, respectively. The baryon and lepton numbers are denoted by \mathbf{B} and \mathbf{L} , respectively. Moreover, L and R subscribes represent left- and right-handed fields.

▲ *Gauge Group* of the minimal left right symmetric interaction (suppressing color) is

$$\mathcal{G} = SU(2)_R \times SU(2)_L \times U(1)_{\mathbf{B}-\mathbf{L}}, \quad (\text{A.1})$$

where (\mathbf{W}_R, g_R) and (\mathbf{W}_L, g_L) are the $SU(2)_R$ and $SU(2)_L$ gauge fields respectively

$$\mathbf{W}_R = W_R^a \mathbf{T}_{aR} \quad \text{and} \quad \mathbf{W}_L = W_L^a \mathbf{T}_{aL}, \quad (\text{A.2})$$

and $(B_\mu, g_{\mathbf{B}-\mathbf{L}})$ is the $U(1)_{\mathbf{B}-\mathbf{L}}$ gauge field which naturally identifies with the $\mathbf{B}-\mathbf{L}$ generator. Here $\mathbf{T}_{L,R}^a$ are the generators of the $SU(2)_{L,R}$

$$\mathbf{T}_{L,R}^a = \frac{\boldsymbol{\tau}_a}{2}, \quad (\text{A.3})$$

where $\boldsymbol{\tau}_a$ denotes the Pauli matrices which acts on the $SU(2)$ -color indices. The $\mathbf{W}_{L,R}$ act on left- and right-handed fields respectively. The strength tensor of $\mathbf{W}_{L,R}$ are given as

$$\mathbf{W}_{\mu\nu} = \partial_\mu \mathbf{W}_\nu - \partial_\nu \mathbf{W}_\mu - ig[\mathbf{W}_\mu, \mathbf{W}_\nu]. \quad (\text{A.4})$$

The electric charge Q is defined as

$$Q = \mathbf{T}_L^3 + \mathbf{T}_R^3 + \frac{\mathbf{B}-\mathbf{L}}{2} = \mathbf{T}_R^3 + Y, \quad (\text{A.5})$$

where Y is the hypercharge.

▲ *Scalar Sector* involves three Higgs fields, i.e. a Higgs bi-doublet to produce the Dirac masses, and two triplet Higgs to create Majorana masses for the neutrinos. The $SU(2)_L \times SU(2)_R$ bi-double with $\mathbf{B}-\mathbf{L}=0$ is

$$\boldsymbol{\Phi} = \begin{pmatrix} \Phi_1^0 & \Phi_2^+ \\ \Phi_1^- & \Phi_2^0 \end{pmatrix}, \quad (\text{A.6})$$

	LRSB Sector	Left-handed	Right-handed
Gauge Fields	$SU(2)_R \times SU(2)_L$	\mathbf{W}_L	\mathbf{W}_R
	$U(1)_{B-L}$	B_μ	
Fermions	quarks	$q_{iL} = \begin{pmatrix} \mathbf{u}_{iL} \\ \mathbf{d}_{iL} \end{pmatrix} : (\mathbf{1}, \mathbf{2}, \frac{1}{3})$	$q_{iR} = \begin{pmatrix} \mathbf{u}_{iR} \\ \mathbf{d}_{iR} \end{pmatrix} : (\mathbf{2}, \mathbf{1}, \frac{1}{3})$
	leptons	$l_{iL} = \begin{pmatrix} \nu_{iL} \\ l_{iL} \end{pmatrix} : (\mathbf{1}, \mathbf{2}, -1)$	$l_{iR} = \begin{pmatrix} \nu_{iR} \\ l_{iR} \end{pmatrix} : (\mathbf{2}, \mathbf{1}, -1)$
Scalars	Higgs $SU(2)$ bi-doublet	$\Phi = \begin{pmatrix} \Phi_1^0 & \Phi_2^+ \\ \Phi_1^- & \Phi_2^0 \end{pmatrix} : (\mathbf{2}, \mathbf{2}, 0)$	
	Higgs $SU(2)$ triplets	$\Delta_L = \begin{pmatrix} \delta^+ & \delta^{++} \\ \delta^0 & -\delta^+ \end{pmatrix}_L : (\mathbf{1}, \mathbf{3}, 2)$	$\Delta_R = \begin{pmatrix} \delta^+ & \delta^{++} \\ \delta^0 & -\delta^+ \end{pmatrix}_R : (\mathbf{3}, \mathbf{1}, 2)$

Table 2. The field content of the minimal Left-Right Symmetric Model (LRSB) extension of the SM.

and the $SU(2)_{R,L}$ triplets with $B - L = 2$ are given as

$$\Delta_{R,L} = \begin{pmatrix} \delta^+ & \delta^{++} \\ \delta^0 & -\delta^+ \end{pmatrix}_{R,L}. \quad (\text{A.7})$$

The gauge-covariant derivatives of Φ and $\Delta_{L,R}$ are given as

$$\mathcal{D}_\mu \Phi = \partial_\mu \Phi - ig_L \mathbf{W}_{\mu L} \Phi + ig_R \Phi \mathbf{W}_{\mu R}, \quad (\text{A.8})$$

$$\mathcal{D}_\mu \Delta_{L,R} = \partial_\mu \Delta_{L,R} - ig_{L,R} [\mathbf{W}_\mu, \Delta]_{L,R} - ig_{BL} B_\mu \Delta_{L,R}. \quad (\text{A.9})$$

The theory of the Higgs sector is given as

$$\begin{aligned} \mathcal{L}_{Higgs} = & -\text{Tr}[(\mathcal{D}_\mu \Delta_R)^\dagger \mathcal{D}^\mu \Delta_R] - \text{Tr}[(\mathcal{D}_\mu \Delta_L)^\dagger \mathcal{D}^\mu \Delta_L] - \text{Tr}[(\mathcal{D}_\mu \Phi)^\dagger \mathcal{D}^\mu \Phi] \\ & - V_{Higgs}(\Phi, \Delta_L, \Delta_R), \end{aligned} \quad (\text{A.10})$$

where the Higgs potential $V_{Higgs}(\Phi, \Delta_R, \Delta_L)$ is the most general renormalizable, gauge and parity invariant potential for Φ and $\Delta_{L,R}$ [7, 69]. The Higgs mass spectrum and the scale of each spontaneous symmetry breaking are given by minimizing the Higgs potential. Here we are interested in the cosmological consequences of such potential. For an exhaustive discussion we refer the interested reader to [8, 70, 71].

▲ *Fermionic Sector* consists of three generations of quarks and leptons as

$$q_{iL,R} = \begin{pmatrix} \mathbf{u}_i \\ \mathbf{d}_i \end{pmatrix}_{L,R} \quad \text{and} \quad l_{iL,R} = \begin{pmatrix} \nu_i \\ l_i \end{pmatrix}_{L,R}, \quad (\text{A.11})$$

where ν_{iR} are three RHNs interacting via the $SU(2)_R$ and $U(1)_{B-L}$. Given that we assume neutrinos are Majorana, and define two Majorana fields associated to the left- and right-handed neutrinos as

$$\nu_i \equiv \nu_{iL} + \nu_{iL}^c \quad \text{and} \quad \mathbf{N}_i \equiv \nu_{iR} + \nu_{iR}^c, \quad (\text{A.12})$$

where the c superscript denotes the charge conjugated field. For simplicity, we present the left- and right-handed fermions collectively as

$$\Psi_{JL,R} = (q_1, q_2, q_3, l_1, l_2, l_3)_{L,R}, \quad (\text{A.13})$$

which are specified by the Lagrangian

$$\mathcal{L}_\Psi = i \sum_{J=1}^6 \bar{\Psi}_{JR} \sigma^\mu \mathcal{D}_\mu \Psi_{JR} + i \bar{\Psi}_{JL} \bar{\sigma}^\mu \mathcal{D}_\mu \Psi_{JL}, \quad (\text{A.14})$$

where the spinor gauge-covariant derivatives are

$$\mathcal{D}_\mu \Psi_{L,R} = (D_\mu - ig_{L,R} \mathbf{W}_{\mu L,R} - \frac{ig_{BL}(B-L)}{2} B_\mu) \Psi_{L,R}, \quad (\text{A.15})$$

$$D_\mu \equiv \partial_\mu + \omega_\mu, \quad (\text{A.16})$$

where ω_μ is the spin connection.¹² For the cosmological background, we have $\sigma^\mu \omega_\mu = \frac{3}{2} H \mathbf{I}_2$ and

$$\sigma^\mu = (\mathbf{I}_2, \frac{1}{a} \sigma_i) \quad \text{and} \quad \bar{\sigma}^\mu = (\mathbf{I}_2, -\frac{1}{a} \sigma_i), \quad (\text{A.17})$$

where σ_i are the Pauli matrices which carries spatial index.¹³ The fermions pick up their mass by the Yukawa interactions

$$\begin{aligned} \mathcal{L}_Y = & -\bar{q}_{iL} (y_{ij}^q \Phi + \tilde{y}_{ij}^q \tilde{\Phi}) q_{jR} - \bar{l}_{iL} (y_{ij}^l \Phi + \tilde{y}_{ij}^l \tilde{\Phi}) l_{jR} - \frac{1}{2} Y_{ij}^R \bar{l}_{iR}^c \tilde{\Delta}_R l_{jR} - \frac{1}{2} Y_{ij}^L \bar{l}_{iL}^c \tilde{\Delta}_L l_{jL} \\ & + h.c., \end{aligned} \quad (\text{A.18})$$

where $l_{Ri}^c = C l_{Ri}^*$ is the charged conjugated l_{Ri} , and

$$\tilde{\Phi} \equiv \tau_2 \Phi^* \tau_2 \quad \text{and} \quad \tilde{\Delta} \equiv i \tau_2 \Delta. \quad (\text{A.19})$$

¹²The spin connection is defined as $\omega_\mu \equiv \frac{i}{2} \omega_{\mu}^{\alpha\beta} \Sigma_{\alpha\beta}$ where $\Sigma_{\alpha\beta} = \frac{i}{4} [\gamma_\alpha, \gamma_\beta]$ and $\omega_{\mu}^{\alpha\beta} \equiv \mathbf{e}^{\alpha\nu} \nabla_\mu \mathbf{e}_\nu^\beta$.

¹³Note that σ_μ is the curved space form of the flat space $\sigma_\alpha = (\mathbf{I}_2, \sigma_i)$ as $\sigma_\mu = e_\mu^\alpha \sigma_\alpha$ where e_μ^α are the tetrads.

Symmetry Breaking Structure, New Fundamental Scale, and Mass:

Once the neutral component of Δ_R acquires a VEV as

$$\langle \Delta_R \rangle = \begin{pmatrix} 0 & 0 \\ \kappa_R & 0 \end{pmatrix}, \quad (\text{A.20})$$

both of the B–L and left-right symmetries are spontaneously broken. That introduces a new fundamental scale, i.e. $\Lambda_F = \kappa_R$, which is much higher than the EW scale, $\Lambda_W \simeq 246 \text{ GeV}$. The 1st SSB breaks the gauge symmetry down to the SM electroweak symmetry as

$$SU(2)_L \times SU(2)_R \times U(1)_{\text{B-L}} \xrightarrow[\Lambda_F]{1^{\text{st}} \text{ SSB}} SU(2)_L \times U(1)_Y. \quad (\text{A.21})$$

All non-Standard Model heavy particle masses are related to the VEV of Δ_R . The charged and neutral $SU(2)_R$ gauge bosons pick up the following masses

$$m_{W_R} = g_R \kappa_R \quad \text{and} \quad m_{Z_R} = \frac{g_{\text{BL}}}{g_Y} m_{W_R}, \quad (\text{A.22})$$

where g_Y is given as

$$g_Y = \frac{g_{\text{BL}} g_R}{\sqrt{g_{\text{BL}}^2 + g_R^2}}. \quad (\text{A.23})$$

The right-handed neutrinos get Majorana mass terms as

$$\mathcal{L}_Y^{\text{SSB1}} = \frac{\kappa_R}{2} Y_{ij}^R \nu_{jR}^T C \nu_{iR} + h.c., \quad (\text{A.24})$$

which leads to the Majorana mass matrix $M_{Rij} = \kappa_R Y_{ij}^R$. Finally, when the temperature drops below the EW phase transition, i.e. $T = \Lambda_W$, the 2nd SSB happens and the neutral components of the bi-doublet receive its VEVs as

$$\langle \Phi \rangle = \frac{1}{\sqrt{2}} \begin{pmatrix} \kappa_1 & 0 \\ 0 & \kappa_2 \end{pmatrix}. \quad (\text{A.25})$$

That breaks the gauge symmetry to $U(1)_{\text{em}}$, i.e.

$$SU(2)_L \times U(1)_Y \xrightarrow[\Lambda_W]{2^{\text{nd}} \text{ SSB}} U(1)_{\text{em}}, \quad (\text{A.26})$$

which provides Dirac masses for the SM particles, SM neutrinos included. After 2nd SSB, therefore, all the SM massive particles pick a Dirac mass similar to SM. The interaction between Δ_R and Φ with Δ_L in Higgs potential imposes a VEV for the latter once the former fields acquired their VEVs. The VEV of Δ_L is of the order of $\mathcal{O}(\frac{\langle \Phi \rangle^2}{\kappa_R}) \ll \langle \Phi \rangle$ [7]. The value of the $\kappa_{1,2}$ is related to the EW scale κ as

$$\kappa_1^2 + \kappa_2^2 = \kappa^2 = (246 \text{ GeV})^2. \quad (\text{A.27})$$

In the limit of our interest, $\kappa_R \gg \kappa_1, \kappa_2, \kappa_L$ in which the left and right charged and neutral gauge bosons are decoupled. Thus, we can consider $W_{L,R}^\pm$ and $Z_{L,R}$ as physical states. Here for simplicity we also assume

$$\kappa_1 \ll \kappa_2 \quad \text{and} \quad \kappa_2 \simeq \kappa.$$

We summarize the symmetry-breaking structure of the setup in Table 3. Below we will discuss its consequences on active neutrinos.

Symmetry Group $SU(2)_R \times SU(2)_L \times U(1)_{B-L}$	After 1st SSB $SU(2)_L \times U(1)_Y$	After 2nd SSB $U(1)_{\text{em}}$
Higgs VEV	$\langle \Delta_R \rangle = \begin{pmatrix} 0 & 0 \\ \kappa_R & 0 \end{pmatrix}$	$\langle \Phi \rangle = \frac{1}{\sqrt{2}} \begin{pmatrix} \kappa_1 & 0 \\ 0 & \kappa_2 \end{pmatrix}$ & $\langle \Delta_L \rangle = \begin{pmatrix} 0 & 0 \\ \kappa_L & 0 \end{pmatrix}$
Massive Particles	W_R^\pm, Z_R and \mathbf{N}_i	SM and ν_i (<i>Seesaw type-I & II</i>)

Table 3. The spontaneous symmetry breaking structure of the minimal LRSM.

Neutrino masses; Natural Seesaw Mechanism:

The first SSB provides Majorana masses for the RHNs and the second SSB gives Dirac masses to neutrinos as well as an induced Majorana mass to left-handed neutrinos. The neutrino mass matrix as

$$M_\nu = \begin{pmatrix} M_L & m_D \\ m_D^T & M_R \end{pmatrix}, \quad (\text{A.28})$$

where the Majorana mass matrices $M_{R,L}$ are

$$M_{Rij} = \kappa_R Y_{ij}^R \quad \text{and} \quad M_{Lij} = \kappa_L Y_{ij}^L \sim \mathcal{O}\left(\frac{\kappa^2}{\kappa_R}\right), \quad (\text{A.29})$$

and the Dirac mass matrix is

$$m_{Dij} = \frac{\kappa}{2} \tilde{y}_{ij}^l. \quad (\text{A.30})$$

Given the fact that $m_D \ll M_R$, we can diagonalize the mass matrix and find the masses of the active neutrinos as

$$m_\nu \approx -m_D^T M_R^{-1} m_D + M_L = \frac{1}{4} \frac{(\kappa^* \tilde{y}^l)^2}{\kappa_R Y^R} + \kappa_L Y^L. \quad (\text{A.31})$$

Note that κ_L is a (small) induced VEV and the contribution of both the first term (seesaw type-I) and the second term (seesaw type-II) are of the same order. Thus, in minimal LRSM, the neutrino mass is a hybrid seesaw type-I, and II [7].

Experimental Constraints on Parameters:

Various Experimental limits can be placed on the mass scales and mixing parameters of the LRSM. First, considering the charged lepton Yukawa couplings as a guide to the neutrino ones suggests $10^{-10} \lesssim \frac{y^2}{Y} \lesssim 1$ which implies a successful seesaw requires

$$10 \text{ TeV} \lesssim \kappa_R \lesssim 10^{15} \text{ GeV}. \quad (\text{A.32})$$

Next, regardless of the details of the SSB, there is a theoretical lower bound on the ratio of g_R to g_L [70]

$$\frac{g_R}{g_L} \geq \tan \theta_w \simeq 0.55. \quad (\text{A.33})$$

That gives $m_{Z_R} \approx 1.7 m_{W_R}$. Finally, there are several constraints for the right-handed charged and neutral gauge boson mass and mixing parameters. These arise due to their direct production or virtual contributions at colliders or astrophysical processes. The $K_L - K_S$ kaon mass difference measurement [64] places a lower bound on the mass of W_R as $m_{W_R} > 1.6 \text{ TeV}$ and the mixing angle between Z_R and Z_L is constrained to be less than 10^{-4} . The possible low-energy W_R has been the target of several LHC collaborations which puts the current bound as $m_{W_R} > 3 \text{ TeV}$ [65]. For an exhaustive discussion of the phenomenological implications and constraints of LRSM, see [66].

Gauge coupling evolution

There is a significant difference between a high scale inflation and electroweak scale. Thus the running of the gauge couplings might be sizable. In the one-loop approximation, the RGE for the $SU(\mathcal{N}_c)$ gauge coupling with \mathcal{N}_f Weyl or Majorana fermions in the fundamental representation and \mathcal{N}_s Higgs fields in the R_s representation is given as

$$\frac{dg_i}{d \ln \left(\frac{k}{\mu} \right)} = b_i \frac{g_i^3}{(4\pi)^2}, \quad (\text{A.34})$$

where k is the momentum, μ is a given scale associated with our renormalization and b_i is

$$b_i = - \left[\frac{11}{3} \mathcal{N}_c - \frac{1}{3} \mathcal{N}_f - \frac{1}{3} \mathcal{N}_s T(R_s) \right]. \quad (\text{A.35})$$

Here $T(R)$ is the index of the irreducible representation $T(R)\delta_{ab} \equiv \text{Tr}(\mathbf{T}_a \mathbf{T}_b)$, where for fields in the fundamental representation of $SU(\mathcal{N}_c)$ it is $T(R_{\text{fund}}) = \frac{1}{2}$ and for the adjoint representation $T(R_{\text{adj}}) = \mathcal{N}_c$. The $SU(2)_L$ and $SU(2)_R$ gauge fields with the Higgs bi-doublet and triplet have $b_{R,L} = -\frac{7}{3}$. Given $g_L(m_{Z_L}) \simeq 0.65$, the RGE determines the L gauge coupling at the GUT scale (assuming inflation happens around GUT, i.e. $k = H \simeq 10^{13} \text{ GeV}$) as

$$g_L(H) \simeq 0.56. \quad (\text{A.36})$$

The gauge coupling of $SU(2)_R$ at the scale of inflation is

$$g_R(H) \simeq 0.56 \frac{g_R(m_{Z_L})}{g_L(m_{Z_L})}. \quad (\text{A.37})$$

Using the theoretical lower bound on g_R in Eq. (A.33), we arrive at

$$0.3 \leq g_R(H) \leq 0.56. \quad (\text{A.38})$$

B Massive Sterile Neutrino production in Inflation

This appendix presents the analytical calculations of massive RHN production by the axion in inflation. In this work, we restrict ourselves to the cases with $\langle \mathbf{W}_R \rangle = 0$.¹⁴ From Eq. (3.46), we find the linearized field equation of ν_{jR} as

$$(i\sigma^\mu \partial_\mu + \frac{3i}{2}H - 2\tilde{\xi}H)\nu_{jR} - m_{N_j}\nu_{jR}^c \simeq 0. \quad (\text{B.1})$$

As a Majorana fermion, $\mathbf{N}_j \equiv \nu_{jR} + \nu_{jR}^c$ can be decomposed as

$$\mathbf{N}_j = \sum_{s=\pm} \frac{1}{a^{\frac{3}{2}}} \int d^3k \left[X_{j\mathbf{k}}^s(\tau) c_{j\mathbf{k}}^s e^{i\mathbf{k}\cdot\mathbf{x}} + Y_{j\mathbf{k}}^s(\tau) c_{j\mathbf{k}}^{s\dagger} e^{-i\mathbf{k}\cdot\mathbf{x}} \right] \mathbf{E}_{\mathbf{k}}^s, \quad (\text{B.2})$$

where $c_{j\mathbf{k}}^s$ and $c_{j\mathbf{k}}^{s\dagger}$ are the annihilation and creation operators of the RHNs as

$$\{c_{i\mathbf{k}}^s, c_{j\mathbf{k}'}^{s'\dagger}\} = \delta^{ss'} \delta_{ij} \delta^{(3)}(\mathbf{k} - \mathbf{k}'), \quad (\text{B.3})$$

and $\mathbf{E}_{\mathbf{k}}^\pm$ are the $\pm\frac{1}{2}$ helicity polarization states

$$\mathbf{E}_{\mathbf{k}}^+ = \frac{k_\alpha \boldsymbol{\sigma}^\alpha}{\sqrt{2k(k+k_3)}} \begin{pmatrix} 1 \\ 0 \end{pmatrix} \quad \text{and} \quad \mathbf{E}_{\mathbf{k}}^- = \frac{k_\alpha \bar{\boldsymbol{\sigma}}^\alpha}{\sqrt{2k(k+k_3)}} \begin{pmatrix} 0 \\ 1 \end{pmatrix}. \quad (\text{B.4})$$

These helicity 2-spinors are the eigenstates of the helicity operator and satisfy $\mathbf{E}_{\mathbf{k}}^{-s} = -is\boldsymbol{\sigma}_2 \mathbf{E}_{\mathbf{k}}^{s*}$. The Majorana condition then requires

$$Y_{j\mathbf{k}}^s = sX_{j\mathbf{k}}^{-s*}. \quad (\text{B.5})$$

The pair of coupled first order differential equations for ν_{iR} and ν_{iR}^c coming from Eq. (B.1) can be decoupled into two second order differential equations for the mode functions $X_{j\mathbf{k}}^\pm(\tau)$. Upon field redefinition

$$\tilde{X}_{j\mathbf{k}}^s \equiv \sqrt{2\tilde{\tau}} X_{j\mathbf{k}}^s, \quad (\text{B.6})$$

we have

$$\partial_{\tilde{\tau}}^2 \tilde{X}_{j\mathbf{k}}^s + \left[1 - \frac{2i\kappa_s}{\tilde{\tau}} + \frac{\frac{1}{4} - \mu_j^2}{\tilde{\tau}^2} \right] \tilde{X}_{j\mathbf{k}}^s = 0, \quad (\text{B.7})$$

¹⁴The fermion production by the Schwinger effect with $\langle \mathbf{W}_R \rangle \neq 0$ in $SU(2)$ -axion inflation is studied in [24].

where κ_s and μ_j are

$$\kappa_s = s\left(\frac{1}{2} + 2i\tilde{\xi}\right) \quad \text{and} \quad \mu_j^2 = -\left(\frac{m_{N_j}}{H}\right)^2 - (2\tilde{\xi})^2. \quad (\text{B.8})$$

Setting the initial conditions with Bunch-Davies vacuum, the solutions are

$$\tilde{X}_{j\mathbf{k}}^+ = \frac{1}{(2\pi)^{\frac{3}{2}}} e^{-\xi\pi} W_{\kappa_+, \mu_j}(-2i\tilde{\tau}), \quad (\text{B.9})$$

$$\tilde{X}_{j\mathbf{k}}^- = -\frac{i}{(2\pi)^{\frac{3}{2}}} \left(\frac{m_{N_j}}{H}\right) e^{\xi\pi} W_{\kappa_-, \mu_j}(-2i\tilde{\tau}). \quad (\text{B.10})$$

Notice that the $-\frac{1}{2}$ helicity mode of the right-handed neutrinos is proportional to their mass. Thus, as we expected, the massless ν_{jR} has only the $+\frac{1}{2}$ helicity state.

Working out the mode functions of the massive sterile neutrinos, we are ready to compute its contribution to the lepton number in Eq. (3.47) as

$$\bar{n}_{N_j} \equiv \int d^3k \langle \nu_{jR}^\dagger \nu_{jR} \rangle = -\frac{\tilde{\xi}}{\pi} \left(\frac{m_{N_j}}{H}\right)^2 H^3 \mathcal{D}(\tilde{\xi}, m_{N_j}). \quad (\text{B.11})$$

Using point splitting regularization, we analytically calculated the above momentum integral in [24].¹⁵ We here use the final result which is

$$\begin{aligned} & \left(\frac{m_{N_j}}{H}\right)^2 \mathcal{D}(\tilde{\xi}, m_{N_j}) = \\ & \frac{1}{2\pi} \left\{ \frac{2}{3} (1 - 2\kappa_I^2) \left(1 - \frac{|\mu_j|}{\kappa_I} \frac{\sinh(2\kappa_I\pi)}{\sinh(2|\mu_j|\pi)}\right) + \frac{m_{N_j}^2}{H^2} \left(2 - 4\psi^{(0)}(1) - \frac{8|\mu_j|}{3\kappa_I} \frac{\sinh(2\kappa_I\pi)}{\sinh(2|\mu_j|\pi)}\right) \right. \\ & \left. + \frac{m_{N_j}^2}{H^2} \sum_{s=\pm} \text{Re} \left[\frac{e^{2|\mu_j|\pi} - e^{-2s\kappa_I\pi}}{\sinh(2|\mu_j|\pi)} \psi^{(0)}(-is\kappa_I - i|\mu_j|) - \frac{e^{-2|\mu_j|\pi} - e^{-2s\kappa_I\pi}}{\sinh(2|\mu_j|\pi)} \psi^{(0)}(-is\kappa_I + i|\mu_j|) \right] \right\}, \end{aligned} \quad (\text{B.12})$$

in which $\kappa_I \equiv 2\tilde{\xi}$ and $\psi^{(0)}(z) \equiv \frac{d\Gamma(z)}{dz}$ is the digamma function.

C Phenomenological Model of Reheating

Reheating starts at some point after the end of inflation and ends at a_{reh} with the formation of a dominant thermal bath with temperature T_{reh} . Yet, the precise physics of reheating is not well understood. Depends on the details of the post-inflation physics, there may be an intermediate phase X with the average equation of state w_X , which connects inflation to the final thermal bath (See Fig. 14). To quantify our analysis and capture these ambiguities, in this appendix, we introduce a phenomenological model for reheating. Next, we compute the entropy injection by the decay of RHNs in our setup.

¹⁵The details of the calculation and point splitting regularization that is used in computing the integral (B.11) can be found in Appendix D of [24]. Notice that κ_+ and κ_- parameters in the current work are denoted as κ_+ and $\tilde{\kappa}_-$ in [24]. The dimensionless parameter ξ_A in the latter is associated with the VEV of the $SU(2)$ gauge field, which is set to zero in the current work.

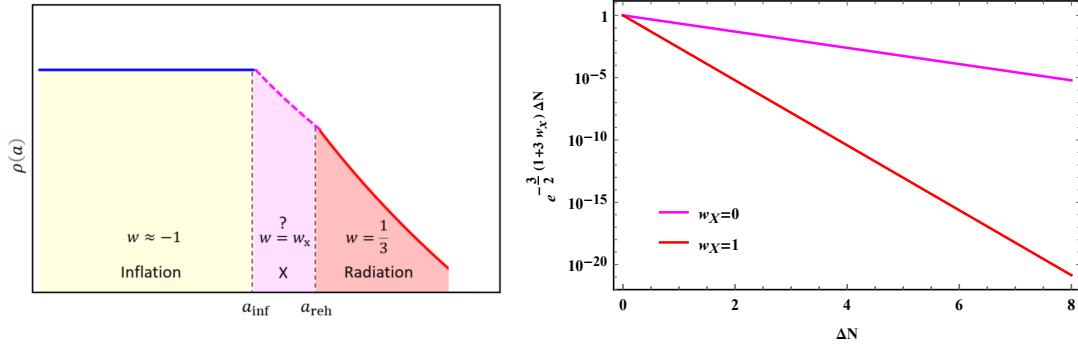


Figure 14. Left Panel: The energy density of Universe vs scale factor. The dashed (pink) line which connects inflation to radiation era is a possible unknown intermediate phase with an average equation of state $w = w_X$. Right Panel: The prefactor $e^{-\frac{3}{2}(1+3w_X)\Delta N}$ in Eq. (4.13) vs $\Delta N = \ln\left(\frac{a_{\text{reh}}}{a_{\text{inf}}}\right)$. (Fig. adopted from ref. [1])

In that case, the energy density at the end of reheating is related to ρ_{inf} as

$$\rho_{\text{reh}} = \delta_{\text{reh}} \rho_{\text{inf}} \left(\frac{a_{\text{inf}}}{a_{\text{reh}}}\right)^4. \quad (\text{C.1})$$

The parameter δ_{reh} is the efficiency of the reheating process

$$\delta_{\text{reh}} \approx \exp\left(- (3w_X - 1)\Delta N\right), \quad (\text{C.2})$$

which models our ignorance about physics of reheating in terms of two parameters; w_X and ΔN given as

$$\Delta N = \ln\left(\frac{a_{\text{reh}}}{a_{\text{inf}}}\right), \quad (\text{C.3})$$

which is the number of e-folds between end of inflation until the formation of the thermal bath. The ratio $\frac{n_{\text{N}}^s}{n_{\text{N}}^p}$ in Eq. (4.13) is related to ΔN as

$$\frac{n_{\text{N}}^s}{n_{\text{N}}^p} \propto e^{-\frac{3}{2}(1+3w_X)\Delta N}. \quad (\text{C.4})$$

Two possible scenarios for the intermediate phase, i.e. X -era in Fig. 14, are: 1) inflation ends in a short period of matter domination with $w_X = 0$ with reheating efficiency parameter as

$$\delta_{\text{reh}} \simeq \left(\frac{a_{\text{reh}}}{a_{\text{inf}}}\right) = e^{\Delta N} > 1, \quad (\text{C.5})$$

which gives

$$\frac{n_{\text{N}}^s}{n_{\text{N}}^p} \propto e^{-\frac{3}{2}\Delta N}, \quad (\text{C.6})$$

or 2) inflation ends with domination of the kinetic term such that $w_X = 1$ and δ_{reh} is

$$\delta_{\text{reh}} \simeq \left(\frac{a_{\text{inf}}}{a_{\text{reh}}}\right)^2 = e^{-2\Delta N} < 1, \quad (\text{C.7})$$

which gives

$$\frac{n_{\mathbf{N}}^s}{n_{\mathbf{N}}^p} \propto e^{-6\Delta N}. \quad (\text{C.8})$$

The factor $e^{-\frac{3}{2}(3w_X+1)\Delta N}$ for these two preheating scenarios are presented in the right panel of Fig. 14.

C.1 Entropy Injection

The out of thermal equilibrium decay of heavy RHNs, i.e. $\mathbf{N}_{2,3}$, at $T = m_{\mathbf{N}_{2,3}}$ injects entropy to the hot plasma and increase the energy of radiation as

$$\rho_{\text{rad}}(a_{\mathbf{N}_i}) = S^{\frac{4}{3}} \left(\frac{a_{\text{reh}}}{a_{\mathbf{N}_i}} \right)^4 \rho_{\text{reh}}, \quad (\text{C.9})$$

where S is the entropy injection factor given as

$$S = 1 + \frac{1}{3} \left(\frac{m_{\mathbf{N}_i}}{M_{\text{Pl}}} \right) \left(\frac{H}{M_{\text{Pl}}} \right) \left(\frac{a_{\mathbf{N}_i}}{a_{\text{reh}}} \right) \left(\frac{n_{\mathbf{N}_i}(a_{\text{reh}})}{\delta_{\text{reh}} H^3} \right), \quad (\text{C.10})$$

where $n_{\mathbf{N}_i}(a_{\text{reh}})$ is the total number density of \mathbf{N}_i , i.e.

$$n_{\mathbf{N}_i} \equiv n_{\mathbf{N}_i}^p + n_{\mathbf{N}_i}^s. \quad (\text{C.11})$$

From Eq. (4.12), the freeze-in part of the density is

$$\frac{n_{\mathbf{N}_i}^s(a_{\text{reh}})}{\delta_{\text{reh}} H^3} \approx 3 \times 10^{11} \exp \left\{ \left[-\frac{(13-3w_X)}{4} \Delta N \right] \right\}, \quad (\text{C.12})$$

while the contribution of the primordial density in Eq. (4.11) gives

$$\frac{n_{\mathbf{N}_i}^p(a_{\text{reh}})}{\delta_{\text{reh}} H^3} \approx \frac{\alpha_{\text{inf}}(\xi)}{3} \exp \{ [-(4-3w_X)\Delta N] \}. \quad (\text{C.13})$$

Given that $\frac{H}{M_{\text{Pl}}} < 10^{-5} \text{ GeV}$ and the mass of the heaviest RHN is around 10^{12} GeV , Eq.s (C.12) implies that contribution of $n_{\mathbf{N}_i}^s$ (freeze-in mechanism) to the entropy injection is negligible in our setup. Therefore, we have

$$S \approx 1 + 10^{-7} \alpha_{\text{inf}}(\xi) \exp \{ [-(4-3w_X)\Delta N] \} \left(\frac{H}{M_{\text{Pl}}} \right). \quad (\text{C.14})$$

In case that the entropy injection is sizable in our setup, the baryon to photon ratio is

$$\eta_{\text{B}}^0 \approx 3 \left(\frac{g_{\text{eff}}}{100} \right)^{\frac{3}{4}} \frac{\alpha_{\text{inf}}(\xi)}{(\delta_{\text{reh}})^{\frac{3}{4}}} \left(\frac{H}{M_{\text{Pl}}} \right)^{\frac{3}{2}}, \quad (\text{C.15})$$

To agree with the data, we need

$$\frac{H}{M_{\text{Pl}}} \approx 10^{-6} \alpha_{\text{inf}}^{-\frac{2}{3}}(\xi) \delta_{\text{reh}}^{\frac{1}{2}} S^{\frac{2}{3}}. \quad (\text{C.16})$$

Combining (C.14) and (C.16), we find a cubic algebraic equation for $S^{\frac{1}{2}}$, i.e.

$$S - A(\xi, \Delta N) S^{\frac{2}{3}} - 1 = 0, \quad (\text{C.17})$$

where $A(\xi, \Delta N)$ is

$$A(\xi, \Delta N) = 10^{-13} \alpha_{\text{inf}}^{\frac{1}{3}}(\xi) \exp \left[-\frac{(7 - 3w_X)}{2} \Delta N \right]. \quad (\text{C.18})$$

The quantity $A(\xi, \Delta N)$ is negligible in the region of our interest (see Fig. 7). Therefore, our setup has negligible entropy injection

$$S \simeq 1. \quad (\text{C.19})$$

D Spectator Effects

This Appendix is devoted to the spectator effects on matter asymmetry. First, we work out the temperature windows in which each of the $W_{L,R}$ sphalerons are in thermal equilibrium and hence can violate the left-/right-handed $\text{B} + \text{L}$. Next, we discuss the lepton flavor effects in our setup.

D.1 $W_{L,R}$ Sphalerons

The $SU(2)_{L,R}$ sphaleron transitions start getting in thermal equilibrium once

$$\frac{\Gamma_{\text{sph}}^{L,R}}{T^3} \gtrsim H(T), \quad (\text{D.1})$$

where $\Gamma_{\text{sph}}^{L,R}$ is the transition rate per unit time per unit volume so dimensional estimate gives $\Gamma_{\text{sph}}^{L,R} \sim (\alpha_{L,R} T)^4$ where $\alpha_{L,R} = \frac{g_{L,R}^2}{4\pi}$. Using lattice simulations the transition rate for the $SU(2)_L$ weak sphalerons has been found in [72] as

$$\Gamma_{\text{sph}}^L = \chi' \alpha_L^5 T^4, \quad (\text{D.2})$$

where $\chi' \approx 18$ and the extra α_L factor is due to specific plasma effects [73]. The $W_{R,L}$ switch off after their corresponding scale of SSB. Therefore, the $SU(2)_L$ weak lepton and baryon violating processes are in thermal equilibrium in the wide temperature interval

$$100 \text{ GeV} < T_{\text{sph}}^L < 10^{12} \text{ GeV}. \quad (\text{D.3})$$

As a rough estimate, we assume that the same relation holds for the $SU(2)_R$ sphalerons, i.e.

$$\Gamma_{\text{sph}}^R \sim \left(\frac{\alpha_R}{\alpha_L} \right)^5 \Gamma_{\text{sph}}^L. \quad (\text{D.4})$$

Thus, W_R sphalerons are in thermal equilibrium in the following interval

$$m_{W_R} \leq T_{\text{sph}}^R \leq \left(\frac{g_R}{g_L} \right)^{10} \times 10^{12} \text{ GeV}. \quad (\text{D.5})$$

Given that in our setup $T_{\text{reh}} < T_{W_R} < m_{W_R}$, the W_R sphalerons are never in equilibrium to cause any $\text{B} + \text{L}$ violating interaction.

D.2 Lepton Flavor Effects

One potentially very significant aspect of leptogenesis is the flavor effects. The flavor-dependent washout and L violating interactions can significantly change the value, and even sign of the final baryon asymmetry [51–53]. By the end of inflation, we have a lepton (anti-lepton) quantum state $|l_{inf}\rangle$ ($|\bar{l}_{inf}\rangle$) as

$$|l_{inf}\rangle \equiv \sum_{\alpha=e,\mu,\tau} C_{\alpha}^{inf} |\alpha\rangle \quad \text{and} \quad |\bar{l}_{inf}\rangle \equiv \sum_{\alpha=e,\mu,\tau} \bar{C}_{\alpha}^{inf} |\alpha\rangle, \quad (\text{D.6})$$

where C_{α}^{inf} and \bar{C}_{α}^{inf} are specified by the physics of inflation as

$$C_{\alpha}^{inf} = \langle \alpha | l_{inf} \rangle \quad \text{and} \quad \bar{C}_{\alpha}^{inf} = \langle \bar{\alpha} | \bar{l}_{inf} \rangle. \quad (\text{D.7})$$

The composition of this primordial initial leptons and their CP conjugated anti-leptons are different. The CP violating decays of the heavy sterile neutrinos can modify these initial states. At very high temperatures $T \gg 10^{12} \text{ GeV}$, however, the interactions are still flavor blind and we can describe leptons as a coherent superposition of charged leptons as

$$|l_i\rangle \equiv \sum_{\alpha=e,\mu,\tau} C_{i\alpha} |\alpha\rangle \quad \text{with} \quad C_{i\alpha} = \langle \alpha | l_i \rangle, \quad (\text{D.8})$$

where $C_{i\alpha}$ are coefficients given by the Yukawa matrix which in terms of the active neutrino mass matrix we have $C_{i\alpha} = \frac{m_{\nu}^{\alpha i}}{\sqrt{(m_{\nu}^{\dagger} m_{\nu})_{\alpha\alpha}}}$. The flavored decay parameters of \mathbf{N}_i to \mathbf{l}_{α} are defined as

$$K_{i\alpha} \equiv \frac{\Gamma(\mathbf{N}_i \rightarrow \Phi^{\dagger} \mathbf{l}_{\alpha}) + \bar{\Gamma}(\mathbf{N}_i \rightarrow \Phi^{\dagger} \mathbf{l}_{\alpha})}{H(T = M_i)} \quad \text{where} \quad \Gamma(\mathbf{N}_i \rightarrow \Phi^{\dagger} \mathbf{l}_{\alpha}) = \frac{M_i Y_{i\alpha}^{\dagger} Y_{\alpha i}}{8\pi}, \quad (\text{D.9})$$

and $K_i = \sum_{\alpha} K_{i\alpha}$. The Yukawa couplings of neutrinos contain several CP-violating phases which remain unconstrained by the current data. Therefore, the decay of sterile neutrinos can be a CP asymmetric process quantified as

$$\varepsilon_{i\alpha} \equiv \frac{\Gamma(\mathbf{N}_i \rightarrow \Phi^{\dagger} \mathbf{l}_{\alpha}) - \bar{\Gamma}(\mathbf{N}_i \rightarrow \Phi^{\dagger} \mathbf{l}_{\alpha})}{\Gamma(\mathbf{N}_i \rightarrow \Phi^{\dagger} \mathbf{l}_{\alpha}) + \bar{\Gamma}(\mathbf{N}_i \rightarrow \Phi^{\dagger} \mathbf{l}_{\alpha})}, \quad (\text{D.10})$$

where $\varepsilon_i = \sum_{\alpha} \varepsilon_{i\alpha}$ is the CP-asymmetry.

In the light of the current neutrino oscillations data, the RH neutrino mass spectrum turns out to be typically highly hierarchical. For the sake of concreteness, in this work, we consider

$$m_{N_3} \gtrsim 10^{12} \text{ GeV} \gg m_{N_2} \gtrsim 10^9 \text{ GeV} \gg m_{N_1}, \quad (\text{D.11})$$

where m_{N_1} is assumed to be lower than the EW scale. Furthermore, we assume that the lightest sterile neutrino has feeble Yukawa interactions with the SM and hence a DM candidate, i.e.

$$K_{1\alpha} \ll 1. \quad (\text{D.12})$$

Therefore, only the two heavy sterile neutrinos, \mathbf{N}_2 and \mathbf{N}_3 contribute to the seesaw mechanism as well as decays and washouts. Moreover, due to the hierarchical neutrino mass spectrum, the decays and washout of \mathbf{N}_2 and \mathbf{N}_3 occur in separate stages with no overlaps. As a result, the decay processes can be studied by the following semi-classical Boltzmann equations for $\eta_X \equiv \frac{n_X}{n_\gamma}$ ($\eta_X^{\text{eq}} = \frac{n_X^{\text{eq}}}{n_\gamma}$)

$$\frac{d\eta_{\mathbf{N}_i}}{dz_i} = -D_i (\eta_{\mathbf{N}_i} - \eta_{\mathbf{N}_i}^{\text{eq}}), \quad (\text{D.13})$$

$$\frac{d\eta_{\delta_i}}{dz_i} = \varepsilon_i D_i (\eta_{\mathbf{N}_i} - \eta_{\mathbf{N}_i}^{\text{eq}}) - W_i \eta_{\delta_i}, \quad (\text{D.14})$$

$$\frac{d\eta_{\delta_{i\perp}}}{dz_i} = 0. \quad (\text{D.15})$$

where $i = 2, 3$, $z_i = \frac{m_{\mathbf{N}_i}}{T}$, and D_i, W_i are the decay, and washout terms, and δ is

$$\delta \equiv \mathbf{B} - \mathbf{L}. \quad (\text{D.16})$$

The decay terms and the related washout terms are given as

$$D_i(z_i) \equiv \frac{\Gamma_i(z_i)}{Hz_i} \quad \text{and} \quad W_i(z_i) \equiv \frac{1}{2} D_i(z_i) \frac{n_{\mathbf{N}_i}^{\text{eq}}(z_i)}{n_{\mathbf{L}}^{\text{eq}}}. \quad (\text{D.17})$$

At very high temperatures $T \gg 10^{12} \text{ GeV}$, the interactions are flavor blind and we can describe leptons as a coherent superposition of charged leptons. At temperatures $10^9 \text{ GeV} < T < 10^{12} \text{ GeV}$, τ lepton-Higgs interactions are fast and destroy the coherence of the lepton states produced by \mathbf{N}_i decay. Therefore the Boltzmann Eq.s (D.14) and (D.15) are effectively described by two incoherent SM flavors, i.e., τ and $\tau^\perp = e + \mu$. The SM lepton asymmetry after decay of \mathbf{N}_2 at $T = M_2 \gtrsim 10^9 \text{ GeV}$ is

$$n_\delta(z_2) = n_\delta^{p,f}(z_2) + n_\delta^{\text{N}}(z_2), \quad (\text{D.18})$$

where $n_\delta^{p,f}(z_2)$ is the contribution of the primordial asymmetry $n_\delta^{p,i}$, as

$$n_\delta^{p,f}(z_2) = \mathcal{C} n_\delta^{p,i} + e^{-\int_1^{z_2} \frac{dW_i(z')}{dz'} dz'} n_{\delta_{3\perp}}^{p,i}, \quad (\text{D.19})$$

and $n_\delta^{\text{N}}(z_2)$ is the lepton number produced by the CP asymmetric decay of \mathbf{N}_2 , i.e.

$$n_\delta^{\text{N}}(z_2) \approx \varepsilon_2 \kappa_2(z_2), \quad (\text{D.20})$$

in which $\kappa_2(z_2)$ is the efficiency factor of the CP asymmetric decay. In this work we are interested in the limit

$$\frac{n_\delta^{\text{N}}(z_2)}{n_\delta^{p,f}} \ll 1 \quad (\text{condition C3}). \quad (\text{D.21})$$

As a result, the SM lepton asymmetry after the washout effects is

$$n_\delta^{p,f} = \mathcal{C} n_\delta^{p,i}. \quad (\text{D.22})$$

For our \mathbf{N}_i mass spectrum given in Eq. (D.11), the decay process consists of two separate stages, which we will study in the following to find the desired \mathcal{C} .

First Stage - decay of \mathbf{N}_3 ($m_{\mathbf{N}_3} \gtrsim 10^{12} \text{ GeV}$):

The decay of \mathbf{N}_3 washes out the pre-existing asymmetry in the direction of heavy neutrino lepton flavor $|l_3\rangle$ while leaves the component normal to it unchanged. The pre-existing asymmetry can be decomposed as

$$n_{\delta}^p = n_{\delta_3}^p + n_{\delta_{3\perp}}^p, \quad (\text{D.23})$$

where $n_{\delta_3}^p$ ($n_{\delta_{3\perp}}^p$) is the asymmetry parallel (perpendicular) to $|l_3\rangle$. The above superposition sum is due to the linearity of the Boltzmann equations. The residual values of the primordial asymmetries are

$$n_{\delta_3}^p = A_3^0 e^{-\frac{3\pi}{8}K_3} n_{\delta}^{p,i} \quad \text{and} \quad n_{\delta_{3\perp}}^p = (1 - A_3^0) n_{\delta}^{p,i}, \quad (\text{D.24})$$

where A_3^0 is the tree-level probability of the primordial asymmetry to be in the direction of $|l_3\rangle$.

Second Stage - decay of \mathbf{N}_2 ($10^{12} \text{ GeV} \gg m_{\mathbf{N}_2} \gtrsim 10^9 \text{ GeV}$):

This stage of our post inflationary evolution can be effectively described by two SM flavors, i.e., $(\tau, \tau^\perp = e + \mu)$ and two relevant flavors of the sterile neutrinos ($\mathbf{N}_2, \mathbf{N}_3$). At temperatures $10^9 \text{ GeV} < T < 10^{12} \text{ GeV}$, τ lepton-Higgs interactions are fast and destroy the coherence of the lepton states produced by \mathbf{N}_i decay. Thus we need to consider separate Boltzmann equations for the components parallel and orthogonal to τ , i.e.

$$n_{\delta_3}^p = n_{\delta_{3\tau}}^p + n_{\delta_{3\tau^\perp}}^p, \quad (\text{D.25})$$

in which

$$n_{\delta_{3\tau}}^p = A_{3\tau}^0 n_{\delta_3}^p \quad \text{and} \quad n_{\delta_{3\tau^\perp}}^p = (1 - A_{3\tau}^0) n_{\delta_3}^p, \quad (\text{D.26})$$

where the probabilities $A_{i\tau}^0$ ($i = 1, 2, 3$) are given in terms of the flavored decay parameters as

$$A_{i\tau}^0 = \frac{K_{i\tau}}{\sum_{\alpha} K_{i\alpha}}. \quad (\text{D.27})$$

From that we can define

$$n_{\delta_\tau}^p \equiv n_{\delta_{3\tau}}^p + n_{\delta_{3\perp\tau}}^p \quad \text{and} \quad n_{\delta_{\tau^\perp}}^p \equiv n_{\delta_{3\tau^\perp}}^p + n_{\delta_{3\perp\tau^\perp}}^p. \quad (\text{D.28})$$

Using Eq. (D.24), we find the explicit form of $n_{\delta_\tau}^p$ and $n_{\delta_{\tau^\perp}}^p$ as

$$n_{\delta_\tau}^p = [A_{3\tau}^0 A_3^0 e^{-\frac{3\pi}{8}K_3} + (1 - A_{3\tau}^0)(1 - A_3^0)] n_{\delta}^{p,i}, \quad (\text{D.29})$$

$$n_{\delta_{\tau^\perp}}^p = [(1 - A_{3\tau}^0) A_3^0 e^{-\frac{3\pi}{8}K_3} + A_{3\tau}^0 (1 - A_3^0)] n_{\delta}^{p,i}. \quad (\text{D.30})$$

At temperatures $T \sim m_{N_2}$, the N_2 wash-out processes act on the flavored asymmetries. The final residual asymmetries in the end of its decay process is

$$n_{\delta_{\tau 2}}^{p,f} = A_{2\tau}^0 e^{-\frac{3\pi}{8} K_2} n_{\delta_{\tau}}^p \quad \text{and} \quad n_{\delta_{\tau 2\perp}}^{p,f} = (1 - A_{2\tau}^0) n_{\delta_{\tau}}^p. \quad (\text{D.31})$$

Similar relations hold for $\tau^\perp = e + \mu$. Fig. 12 shows the geometrical structure of the flavor effects in the flavor space.

The final residual asymmetry in the SM lepton frame is

$$n_{\delta_{\tau}}^{p,f} = A_{2\tau}^0 e^{-\frac{3\pi}{8} K_2} n_{\delta_{\tau}}^p + (1 - A_{2\tau}^0) n_{\delta_{\tau}}^p, \quad (\text{D.32})$$

$$n_{\delta_{\tau\perp}}^{p,f} = (1 - A_{2\tau}^0) e^{-\frac{3\pi}{8} K_2} n_{\delta_{\tau\perp}}^p + A_{2\tau}^0 n_{\delta_{\tau\perp}}^p. \quad (\text{D.33})$$

Considering the most conservative assumption that the decaying terms experience strong washout effects and are negligible, the final remnant of the primordial (inflationary) asymmetry is

$$n_{\delta}^{p,f} = n_{\delta_{\tau}}^{p,f} + n_{\delta_{\tau\perp}}^{p,f} = \mathcal{C} n_{\delta}^{p,i}, \quad (\text{D.34})$$

where \mathcal{C} is

$$\mathcal{C} \simeq (1 - A_3^0)(1 - A_{2\tau}^0 - A_{3\tau}^0 + 2A_{2\tau}^0 A_{3\tau}^0). \quad (\text{D.35})$$

Fig. 15 presents

$$\mathcal{A}_f \equiv (1 - A_{2\tau}^0 - A_{3\tau}^0 + 2A_{2\tau}^0 A_{3\tau}^0). \quad (\text{D.36})$$

vs $A_{2\tau}^0$ and $A_{3\tau}^0$ where the dark shaded area denotes regions with $\mathcal{A}_f < 0.1$. As we see, in most of its parameter space, \mathcal{A}_f is close to one with an average value as

$$\bar{\mathcal{A}}_f = \frac{1}{2}. \quad (\text{D.37})$$

Given that our inflationary primordial asymmetry is flavor blind, it is a plausible assumption to consider $A_3^0 = \frac{1}{3}$. For typical values of flavored decay rates, the remnant of the primordial asymmetry is significant which is related to the inflationary asymmetry as

$$\frac{1}{3} \lesssim \mathcal{C} = \frac{n_{\delta}^{p,f}}{n_{\delta}^{p,i}} < 1. \quad (\text{D.38})$$

Interestingly, eliminating the effect of this pre-existing asymmetry requires tightly fine-tuned relations between the flavored decay rates, hence on leptonic Yukawa couplings, and the flavor-space direction of the inflationary asymmetry. More precisely, one needs either i) $|l_{inf}\rangle$ coincides with one of $|l_2\rangle$ and $|l_3\rangle$, or ii) $|l_2\rangle$ and $|l_3\rangle$ are perpendicular to each other which $|l_{inf}\rangle$ is in the plane of $|l_2\rangle - |l_3\rangle$. As a result, the relation presented in Eq. (D.38) is a good estimate for most of the possible flavor parameter space.

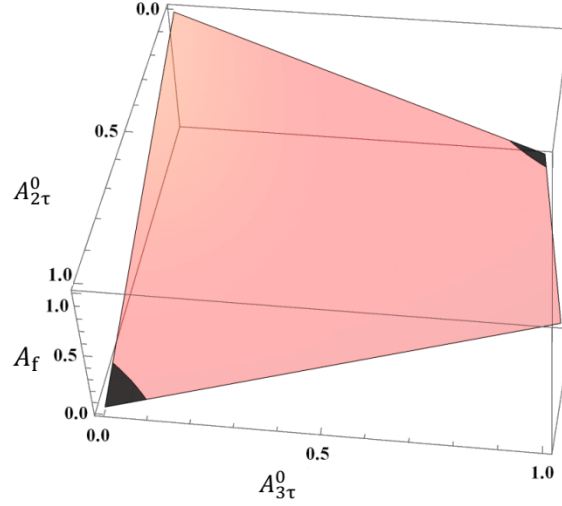


Figure 15. The flavor parameter \mathcal{A}_f in terms of $A_{2\tau}^0$ and $A_{3\tau}^0$. The dark shaded area shows regions with $\mathcal{A}_f < 0.1$.

References

- [1] A. Maleknejad, *SU(2)_R and its Axion in Cosmology: A common Origin for Inflation, Cold Sterile Neutrinos, and Baryogenesis*, [2012.11516](#).
- [2] J. C. Pati and A. Salam, *Lepton Number as the Fourth Color*, *Phys. Rev. D* **10** (1974) 275.
- [3] R. Mohapatra and J. C. Pati, *A Natural Left-Right Symmetry*, *Phys. Rev. D* **11** (1975) 2558.
- [4] G. Senjanovic and R. N. Mohapatra, *Exact Left-Right Symmetry and Spontaneous Violation of Parity*, *Phys. Rev. D* **12** (1975) 1502.
- [5] A. Davidson, , *Phys. Rev. D* **20** (1979) 776.
- [6] R. N. Mohapatra and R. Marshak, *Local B-L Symmetry of Electroweak Interactions, Majorana Neutrinos and Neutron Oscillations*, *Phys. Rev. Lett.* **44** (1980) 1316.
- [7] R. N. Mohapatra and G. Senjanovic, *Neutrino Masses and Mixings in Gauge Models with Spontaneous Parity Violation*, *Phys. Rev. D* **23** (1981) 165.
- [8] A. Maiezza, G. Senjanović and J. C. Vazquez, *Higgs sector of the minimal left-right symmetric theory*, *Phys. Rev. D* **95** (2017) 095004 [[1612.09146](#)].
- [9] K. Freese, J. A. Frieman and A. V. Olinto, *Natural inflation with pseudo - Nambu-Goldstone bosons*, *Phys. Rev. Lett.* **65** (1990) 3233.
- [10] E. Pajer and M. Peloso, *A review of Axion Inflation in the era of Planck*, *Class. Quant. Grav.* **30** (2013) 214002 [[1305.3557](#)].
- [11] L. McAllister, E. Silverstein, A. Westphal and T. Wrase, *The Powers of Monodrom*, *JHEP* **09** (2014) 123 [[1405.3652](#)].
- [12] A. Maleknejad and M. Sheikh-Jabbari, *Non-Abelian Gauge Field Inflation*, *Phys. Rev. D* **84** (2011) 043515 [[1102.1932](#)].
- [13] A. Maleknejad and M. Sheikh-Jabbari, *Gauge-flation: Inflation From Non-Abelian Gauge Fields*, *Phys. Lett. B* **723** (2013) 224 [[1102.1513](#)].

- [14] P. Adshead and M. Wyman, *Chromo-Natural Inflation: Natural inflation on a steep potential with classical non-Abelian gauge fields*, *Phys. Rev. Lett.* **108** (2012) 261302 [[1202.2366](#)].
- [15] M. Sheikh-Jabbari, *Gauge-flation Vs Chromo-Natural Inflation*, *Phys. Lett. B* **717** (2012) 6 [[1203.2265](#)].
- [16] D. Baumann and L. McAllister, *Inflation and String Theory*, Cambridge Monographs on Mathematical Physics. Cambridge University Press, 5, 2015, [10.1017/CBO9781316105733](#), [[1404.2601](#)].
- [17] A. Maleknejad, *Axion Inflation with an $SU(2)$ Gauge Field: Detectable Chiral Gravity Waves*, *JHEP* **07** (2016) 104 [[1604.03327](#)].
- [18] A. Maleknejad, M. Sheikh-Jabbari and J. Soda, *Gauge Fields and Inflation*, *Phys. Rept.* **528** (2013) 161 [[1212.2921](#)].
- [19] A. Maleknejad and E. Komatsu, *Production and Backreaction of Spin-2 Particles of $SU(2)$ Gauge Field during Inflation*, *JHEP* **05** (2019) 174 [[1808.09076](#)].
- [20] M. Bastero-Gil, A. Berera, R. O. Ramos and J. G. Rosa, *Warm Little Inflaton*, *Phys. Rev. Lett.* **117** (2016) 151301 [[1604.08838](#)].
- [21] V. Kamali, *Warm pseudoscalar inflation*, *Phys. Rev. D* **100** (2019) 043520 [[1901.01897](#)].
- [22] K. V. Berghaus, P. W. Graham and D. E. Kaplan, *Minimal Warm Inflation*, *JCAP* **03** (2020) 034 [[1910.07525](#)].
- [23] K. D. Lozanov, A. Maleknejad and E. Komatsu, *Schwinger Effect by an $SU(2)$ Gauge Field during Inflation*, *JHEP* **02** (2019) 041 [[1805.09318](#)].
- [24] A. Maleknejad, *Dark Fermions and Spontaneous CP violation in $SU(2)$ -axion Inflation*, *JHEP* **07** (2020) 154 [[1909.11545](#)].
- [25] L. Mirzaghali, A. Maleknejad and K. D. Lozanov, *Production and backreaction of fermions from axion- $SU(2)$ gauge fields during inflation*, *Phys. Rev. D* **101** (2020) 083528 [[1905.09258](#)].
- [26] A. Sakharov, *Violation of CP Invariance, C asymmetry, and baryon asymmetry of the universe*, *Sov. Phys. Usp.* **34** (1991) 392.
- [27] A. Maleknejad, *Chiral Gravity Waves and Leptogenesis in Inflationary Models with non-Abelian Gauge Fields*, *Phys. Rev. D* **90** (2014) 023542 [[1401.7628](#)].
- [28] A. Maleknejad, *Gravitational leptogenesis in axion inflation with $SU(2)$ gauge field*, *JCAP* **12** (2016) 027 [[1604.06520](#)].
- [29] R. Caldwell and C. Devulder, *Axion Gauge Field Inflation and Gravitational Leptogenesis: A Lower Bound on B Modes from the Matter-Antimatter Asymmetry of the Universe*, *Phys. Rev. D* **97** (2018) 023532 [[1706.03765](#)].
- [30] S. Alexander, E. McDonough and D. N. Spergel, *Chiral Gravitational Waves and Baryon Superfluid Dark Matter*, *JCAP* **05** (2018) 003 [[1801.07255](#)].
- [31] P. Adshead, E. Martinec and M. Wyman, *Gauge fields and inflation: Chiral gravitational waves, fluctuations, and the Lyth bound*, *Phys. Rev. D* **88** (2013) 021302 [[1301.2598](#)].
- [32] E. Dimastrogiovanni and M. Peloso, *Stability analysis of chromo-natural inflation and possible evasion of Lyth's bound*, *Phys. Rev. D* **87** (2013) 103501 [[1212.5184](#)].

- [33] A. Agrawal, T. Fujita and E. Komatsu, *Tensor Non-Gaussianity from Axion-Gauge-Fields Dynamics : Parameter Search*, *JCAP* **06** (2018) 027 [[1802.09284](#)].
- [34] P. Campeti, E. Komatsu, D. Poletti and C. Baccigalupi, *Measuring the spectrum of primordial gravitational waves with CMB, PTA and Laser Interferometers*, [2007.04241](#).
- [35] B. Thorne, T. Fujita, M. Hazumi, N. Katayama, E. Komatsu and M. Shiraishi, *Finding the chiral gravitational wave background of an axion- $SU(2)$ inflationary model using CMB observations and laser interferometers*, *Phys. Rev. D* **97** (2018) 043506 [[1707.03240](#)].
- [36] E. Silverstein and A. Westphal, *Monodromy in the CMB: Gravity Waves and String Inflation*, *Phys. Rev. D* **78** (2008) 106003 [[0803.3085](#)].
- [37] R. Flauger, L. McAllister, E. Pajer, A. Westphal and G. Xu, *Oscillations in the CMB from Axion Monodromy Inflation*, *JCAP* **06** (2010) 009 [[0907.2916](#)].
- [38] P. Adshead, E. Martinec, E. I. Sfakianakis and M. Wyman, *Higgsed Chromo-Natural Inflation*, *JHEP* **12** (2016) 137 [[1609.04025](#)].
- [39] P. Adshead and E. I. Sfakianakis, *Higgsed Gauge-flation*, *JHEP* **08** (2017) 130 [[1705.03024](#)].
- [40] R. Peccei and H. R. Quinn, *CP Conservation in the Presence of Instantons*, *Phys. Rev. Lett.* **38** (1977) 1440.
- [41] S. Weinberg, *The quantum theory of fields. Vol. 2: Modern applications*. Cambridge University Press, 8, 2013.
- [42] S. L. Adler, *Axial vector vertex in spinor electrodynamics*, *Phys. Rev.* **177** (1969) 2426.
- [43] J. Bell and R. Jackiw, *A PCAC puzzle: $\pi^0 \rightarrow \gamma\gamma$ in the σ model*, *Nuovo Cim. A* **60** (1969) 47.
- [44] M. Nemevsek, G. Senjanovic and Y. Zhang, *Warm Dark Matter in Low Scale Left-Right Theory*, *JCAP* **07** (2012) 006 [[1205.0844](#)].
- [45] BICEP2, KECK ARRAY collaboration, P. A. R. Ade et al., *BICEP2 / Keck Array x: Constraints on Primordial Gravitational Waves using Planck, WMAP, and New BICEP2/Keck Observations through the 2015 Season*, *Phys. Rev. Lett.* **121** (2018) 221301 [[1810.05216](#)].
- [46] D. Dunsky, L. J. Hall and K. Harigaya, *Sterile Neutrino Dark Matter and Leptogenesis in Left-Right Higgs Parity*, [2007.12711](#).
- [47] T. G. Rizzo and G. Senjanovic, *Can There Be Low Intermediate Mass Scales in Grand Unified Theories?*, *Phys. Rev. Lett.* **46** (1981) 1315.
- [48] S. Bertolini, L. Di Luzio and M. Malinsky, *Seesaw Scale in the Minimal Renormalizable $SO(10)$ Grand Unification*, *Phys. Rev. D* **85** (2012) 095014 [[1202.0807](#)].
- [49] F. F. Deppisch, T. E. Gonzalo and L. Graf, *Surveying the $SO(10)$ Model Landscape: The Left-Right Symmetric Case*, *Phys. Rev. D* **96** (2017) 055003 [[1705.05416](#)].
- [50] D. Bödeker and D. Schröder, *Kinetic equations for sterile neutrinos from thermal fluctuations*, *JCAP* **02** (2020) 033 [[1911.05092](#)].
- [51] A. Abada, S. Davidson, F.-X. Josse-Michaux, M. Losada and A. Riotto, *Flavor issues in leptogenesis*, *JCAP* **04** (2006) 004 [[hep-ph/0601083](#)].
- [52] R. Barbieri, P. Creminelli, A. Strumia and N. Tetradis, *Baryogenesis through leptogenesis*, *Nucl. Phys. B* **575** (2000) 61 [[hep-ph/9911315](#)].

- [53] S. Blanchet, P. Di Bari and G. Raffelt, *Quantum Zeno effect and the impact of flavor in leptogenesis*, *JCAP* **03** (2007) 012 [[hep-ph/0611337](#)].
- [54] E. Bertuzzo, P. Di Bari and L. Marzola, *The problem of the initial conditions in flavoured leptogenesis and the tauon N_2 -dominated scenario*, *Nucl. Phys. B* **849** (2011) 521 [[1007.1641](#)].
- [55] P. Di Bari and L. Marzola, *$SO(10)$ -inspired solution to the problem of the initial conditions in leptogenesis*, *Nucl. Phys. B* **877** (2013) 719 [[1308.1107](#)].
- [56] M. Fukugita and T. Yanagida, *Baryogenesis Without Grand Unification*, *Phys. Lett. B* **174** (1986) 45.
- [57] PLANCK collaboration, P. Ade et al., *Planck 2015 results. XIII. Cosmological parameters*, *Astron. Astrophys.* **594** (2016) A13 [[1502.01589](#)].
- [58] P. B. Pal and L. Wolfenstein, *Radiative Decays of Massive Neutrinos*, *Phys. Rev. D* **25** (1982) 766.
- [59] V. D. Barger, R. Phillips and S. Sarkar, *Remarks on the KARMEN anomaly*, *Phys. Lett. B* **352** (1995) 365 [[hep-ph/9503295](#)].
- [60] FERMI-LAT collaboration, M. Ackermann et al., *Search for Gamma-ray Spectral Lines with the Fermi Large Area Telescope and Dark Matter Implications*, *Phys. Rev. D* **88** (2013) 082002 [[1305.5597](#)].
- [61] A. Lue, L.-M. Wang and M. Kamionkowski, *Cosmological signature of new parity violating interactions*, *Phys. Rev. Lett.* **83** (1999) 1506 [[astro-ph/9812088](#)].
- [62] S. Saito, K. Ichiki and A. Taruya, *Probing polarization states of primordial gravitational waves with CMB anisotropies*, *JCAP* **09** (2007) 002 [[0705.3701](#)].
- [63] C. R. Contaldi, J. Magueijo and L. Smolin, *Anomalous CMB polarization and gravitational chirality*, *Phys. Rev. Lett.* **101** (2008) 141101 [[0806.3082](#)].
- [64] G. Barenboim, J. Bernabeu, J. Prades and M. Raidal, *Constraints on the W_R mass and CP violation in left-right models*, *Phys. Rev. D* **55** (1997) 4213 [[hep-ph/9611347](#)].
- [65] S. Bertolini, A. Maiezza and F. Nesti, *Present and Future K and B Meson Mixing Constraints on TeV Scale Left-Right Symmetry*, *Phys. Rev. D* **89** (2014) 095028 [[1403.7112](#)].
- [66] PARTICLE DATA GROUP collaboration, J. Beringer et al., *Review of Particle Physics (RPP)*, *Phys. Rev. D* **86** (2012) 010001.
- [67] H.E.S.S. collaboration, A. Abramowski et al., *Search for Photon-Linelike Signatures from Dark Matter Annihilations with H.E.S.S.*, *Phys. Rev. Lett.* **110** (2013) 041301 [[1301.1173](#)].
- [68] J. Aleksić et al., *Optimized dark matter searches in deep observations of Segue 1 with MAGIC*, *JCAP* **02** (2014) 008 [[1312.1535](#)].
- [69] N. Deshpande, J. Gunion, B. Kayser and F. I. Olness, *Left-right symmetric electroweak models with triplet Higgs*, *Phys. Rev. D* **44** (1991) 837.
- [70] P. S. B. Dev, R. N. Mohapatra and Y. Zhang, *Probing the Higgs Sector of the Minimal Left-Right Symmetric Model at Future Hadron Colliders*, *JHEP* **05** (2016) 174 [[1602.05947](#)].
- [71] P. Bhupal Dev, R. N. Mohapatra, W. Rodejohann and X.-J. Xu, *Vacuum structure of the left-right symmetric model*, *JHEP* **02** (2019) 154 [[1811.06869](#)].

- [72] D. Bodeker, G. D. Moore and K. Rummukainen, *Hard thermal loops and the sphaleron rate on the lattice*, *Nucl. Phys. B Proc. Suppl.* **83** (2000) 583 [[hep-lat/9909054](#)].
- [73] P. B. Arnold, D. Son and L. G. Yaffe, *The Hot baryon violation rate is $O(\alpha_w^5 T^4)$* , *Phys. Rev. D* **55** (1997) 6264 [[hep-ph/9609481](#)].